Molecular Pharmacology Fast Forward. Published on December 2, 2020 as DOI: 10.1124/molpharm.120.000106
This article has not been copyedited and formatted. The final version may differ from this version.

Title Page

Identification and Characterization of a Novel BK_{Ca} Channel Activator, CTIBD, and Its Relaxation Effect on Urinary Bladder Smooth Muscle

Narasaem Lee, Bong Hee Lim, Kyu-Sung Lee, Jimin Shin, Haushabhau S. Pagire, Suvarna H. Pagire, Jin Hee Ahn, Sung Won Lee, Tong Mook Kang, and Chul-Seung Park*

School of Life Sciences, Center for AI-applied High Efficiency Drug Discovery and Integrated Institute of Biomedical Research, Gwangju Institute of Science and Technology (GIST), Gwangju (N.L., C.-S.P.); Department of Urology, Samsung Medical Center, Samsung Biomedical Research Institute, Sungkyunkwan University School of Medicine, Seoul (B.H.L., J.S., K.-S.L., S.W.L.); Department of Physiology, Sungkyunkwan University School of Medicine, Suwon (T.M.K.); Department of Chemistry, Gwangju Institute of Science and Technology (GIST), Gwangju (H.S.P., S.H.P., J.H.A.), Republic of Korea

This work was supported by the Korea Institute of Planning and Evaluation for Technology in Food, Agriculture, and Forestry (IPET) through the Agri-Bio Industry Technology Development Program, funded by the Ministry of Agriculture, Food and Rural Affairs (MAFRA) (317070-4) and supported by GIST Research Institute (GRI) IIBR grant funded in 2020.

Downloaded from molpharm.aspetjournals.org at ASPET Journals on April 20, 2024

Molecular Pharmacology Fast Forward. Published on December 2, 2020 as DOI: 10.1124/molpharm.120.000106
This article has not been copyedited and formatted. The final version may differ from this version.

Running Title Page

Bladder Relaxation Effect of BK_{Ca} Channel Activator, CTIBD

***Corresponding Author**

Chul-Seung Park

School of Life Sciences, Center for AI-applied High Efficiency Drug Discovery, and Integrated Institute of Biomedical Research, Gwangju Institute of Science and Technology (GIST), 123, Cheomdangwagi-ro, Buk-gu, Gwangju, Republic of Korea

Tel.: 82-62-715-2489

Fax number : 82-62-715-2484

E-mail Adress : cspark@gist.ac.kr

The number of text pages : 29

The number of figures : 10

The number of references : 34

The number of words in the abstract : 235

The number of words in the introduction : 632

The number of words in the discussion : 1,051

Downloaded from molpharm.aspetjournals.org at ASPET Journals on April 20, 2024

Molecular Pharmacology Fast Forward. Published on December 2, 2020 as DOI: 10.1124/molpharm.120.000106
This article has not been copyedited and formatted. The final version may differ from this version.

Abbreviations

AA, acetic acid; ACh, acetylcholine; BK_{Ca} channel, large-conductance calcium-activated potassium channel; cRNA, complementary RNA; CTIBD, 4-(4-(4-chlorophenyl)-3-(trifluoromethyl)isoxazol-5-yl)benzene-1,3-diol; DMSO, dimethyl sulfoxide; *G*–*V*, conductance–voltage; G_{max}, maximum conductance; HEK293, human embryonic kidney 293; OAB, overactive bladder; p_o, open probability; RFU, relative fluorescence unit; UBSM, urinary bladder smooth muscle; $V_{1/2}$, half-activation voltage.

Downloaded from molpharm.aspetjournals.org at ASPET Journals on April 20, 2024

Molecular Pharmacology Fast Forward. Published on December 2, 2020 as DOI: 10.1124/molpharm.120.000106
This article has not been copyedited and formatted. The final version may differ from this version.

Abstract

The BK_{Ca} channel (large-conductance calcium-activated potassium channel) is expressed on various tissues and is involved in smooth muscle relaxation. The channel is highly expressed on urinary bladder smooth muscle (UBSM) cells and regulates the repolarization phase of the spontaneous action potentials that control muscle contraction. To discover novel chemical activators of the BK_{Ca} channel, we screened a chemical library containing 8,364 chemical compounds using a cell-based fluorescence assay. A chemical compound containing an isoxazolyl benzene skeleton (compound 1) was identified as a potent activator of the BK_{Ca} channel and was structurally optimized through a structure–activity relationship study to obtain 4-(4-(4-chlorophenyl)-3-(trifluoromethyl)isoxazol-5-yl)benzene-1,3-diol (CTIBD). When CTIBD was applied to the treated extracellular side of the channel, the conductance–voltage relationship of the channel shifted toward a negative value, and the maximum conductance increased in a concentration-dependent manner. CTIBD altered the gating kinetics of the channel by dramatically slowing channel closing without effecting channel opening. The effects of CTIBD on bladder muscle relaxation and micturition function were tested in rat tissue and *in vivo*. CTIBD concentration-dependently reduced acetylcholine-induced contraction of urinary bladder smooth muscle strips. In an acetic acid-induced overactive bladder (OAB) model, intraperitoneal injection of 20 mg/kg CTIBD effectively restored frequent voiding contraction and lowered voiding volume without affecting other bladder function parameters. Thus, our results indicate that CTIBD and its derivatives are novel chemical activators of the bladder BK_{Ca} channel and potential candidates for OAB therapeutics.

Significance Statement

Novel BK_{Ca} channel activator, CTIBD, was identified and characterized at this study. CTIBD directly activate BK_{Ca} channel and relax urinary bladder smooth muscle of rat, so CTIBD can be a potential candidate for OAB therapeutics.

Downloaded from molpharm.aspetjournals.org at ASPET Journals on April 20, 2024

Molecular Pharmacology Fast Forward. Published on December 2, 2020 as DOI: 10.1124/molpharm.120.000106
This article has not been copyedited and formatted. The final version may differ from this version.

Introduction

The large-conductance Ca^{2+}-activated K^+ channel (BK_{Ca} channel; also called Maxi K, Slo 1, or K_{Ca} 1.1) is activated by membrane depolarization or increases in intracellular Ca^{2+} concentration (Barrett et al., 1982; Yang et al., 2015). Potassium ions pass through the channel rapidly from the intracellular side to the extracellular side when the BK_{Ca} channel is opened, resulting in membrane hyperpolarization (Cui et al., 2009; Salkoff et al., 2006). The BK_{Ca} channel is composed of four pore-forming α-subunits and auxiliary β-subunits. Four types of β-subunits, β1–β4, show tissue-specific distributions and affect the activation of BK_{Ca} channels (Orio et al., 2002). The BK_{Ca} channel is expressed in the brain, smooth muscle, bladder, cochlea and other various tissues (Poulsen et al., 2009). The BK_{Ca} channel regulates several physiological processes; for example, neurotransmitter release (Wang, 2008), smooth muscle contraction (Wu and Marx, 2010), hormone secretion from endocrine cells (Marty, 1981; Wang et al., 1994), hearing (Salkoff et al., 2006), and circadian rhythms (Meredith et al., 2006). Based on these roles, malfunction of the BK_{Ca} channel is linked to several diseases such as stroke (Gribkoff et al., 2001), erectile dysfunction (Werner et al., 2005), and overactive bladder (OAB) (Layne et al., 2010). In addition, a gain-of-function mutation of BK_{Ca} channel was linked to epilepsy and paroxysmal dyskinesia (Du et al., 2005).

OAB syndrome makes patients feel frequent urinary urgency both day and night (Cerruto et al., 2012). In the United States, 16.0 % of men and 16.9 % of women suffer from OAB (Stewart et al., 2003). In the urination pathway, acetylcholine (ACh) released from parasympathetic nerves binds to muscarinic receptors on urinary bladder smooth muscle (UBSM) to induce contraction of UBSM and urination (Hegde and Eglen, 1999). Muscarinic receptor antagonists, which inhibit ACh-induced UBSM contraction, are commonly used to treat OAB (Abrams and Andersson, 2007). However, these induce several side effects such as blurred vision, dry mouth, constipation, tachycardia, and cognitive impairment (Eglen et al., 1999; Kay and Granville, 2005). Therefore, different therapeutic targets for OAB syndrome that are associated with fewer side effects need to be studied.

As aforementioned, the BK_{Ca} channel controls smooth muscle contraction (Wu and Marx,

Downloaded from molpharm.aspetjournals.org at ASPET Journals on April 20, 2024

Molecular Pharmacology Fast Forward. Published on December 2, 2020 as DOI: 10.1124/molpharm.120.000106
This article has not been copyedited and formatted. The final version may differ from this version.

2010). The BK_{Ca} channel is highly expressed in UBSM cells (Hristov et al., 2011), where it maintains the resting membrane potential and regulates the repolarization phase of the spontaneous action potential that controls UBSM contraction (Petkov, 2014). Cholinergic- and purinergic-induced contractility is decreased by BK_{Ca} channel activation, and alterations in BK_{Ca} channel expression or function affect OAB symptoms (Sprossmann et al., 2009; Werner et al., 2007). Thus, UBSM relaxation can be induced by BK_{Ca} channel activation, suggesting that the BK_{Ca} channel is a potential therapeutic target for the treatment of OAB.

In this study, we screened 8,364 chemical compounds using a cell-based fluorescence assay to search for a novel BK_{Ca} channel activator. A thallium (TI^+)-based fluorescence assay platform, which measures the activity of voltage-gated K^+ channels, was used for screening the activity of the compounds against a mutant BK_{Ca} channel. The channel has highly increased sensitivity to Ca^{2+}, meaning an increase in intracellular Ca^{2+} concentration is not required for channel activation (Lee et al., 2013). From the initial screening and the secondary structure–activity relationship study, we identified one chemical compound, 4-(4-(4-chlorophenyl)-3-(trifluoromethyl)isoxazol-5-yl)benzene-1,3-diol (CTIBD), as a potent activator of the BK_{Ca} channel. The conductance–voltage (*G*–*V*) relationship of the BK_{Ca} channel shifted to a more negative value in a concentration-dependent manner when CTIBD was applied to the extracellular side of the channel. In addition, CTIBD significantly decreased ACh-induced contraction of rat UBSM strips (Bo and Burnstock, 1990). When injected intraperitoneally into a rat model of acetic acid (AA)-induced OAB, CTIBD increased the reduced inter-contraction interval and voiding volume significantly. Thus, CTIBD and its derivatives may hold potential as OAB therapeutics that target the BK_{Ca} channel.

Downloaded from molpharm.aspetjournals.org at ASPET Journals on April 20, 2024

Molecular Pharmacology Fast Forward. Published on December 2, 2020 as DOI: 10.1124/molpharm.120.000106
This article has not been copyedited and formatted. The final version may differ from this version.

Materials and Methods

Materials. A chemical library, named KRICT Diversity Library, which contains 8,364 unique chemical compounds, was obtained from the Korea Research Institute of Chemical Technology (KRICT, Daejon, South Korea; www.chembank.org). 4-(4-(4-chlorophenyl)-3-(trifluoromethyl)isoxazol-5-yl)benzene-1,3-diol (CTIBD) and other isoxazolyl benzene derivatives were purchased from Vitas-M Laboratory at first (Causeway Bay, Hong Kong; www.vitasmlab.biz). After that, large amount of CTIBD and its derivatives were synthesized (Suppl. Fig. 1). Those compounds are prepared by dissolving compounds in dimethyl sulfoxide (DMSO; Sigma-Aldrich, St. Louis, MO).

Synthesis of Compound 4 (CTIBD). Compound 4 (CTIBD) was synthesized as outlined in Scheme 1 and synthetic procedure as follows: 2-(4-Chlorophenyl)-1-(2,4-dihydroxyphenyl)ethan-1-one **3**: To a solution of resorcinol **1** (1.42 g, 12.89 mmol) in $BF_3.Et_2O$ (20 mL) was added 2-(4-chlorophenyl) acetic acid **2** (2 g, 11.72 mmol), and the reaction mixture was heated at 75 °C for 4 hours under a nitrogen atmosphere. The mixture was poured into water and extracted with EtOAc. The organic layer was separated, dried over anhydrous Na_2SO_4, filtered, and concentrated *in vacuo*. Purification of the resulting residue by column chromatography using EtOAc/hexane as the eluent provided 2-(4-chlorophenyl)-1-(2,4-dihydroxyphenyl)ethan-1-one **3** (1.7 g, 55% yield). Characterization of **3**: ^{1}H NMR (DMSO-d_6) δ 12.40 (s, 1H), 10.69 (s, 1H), 7.93 (d, J = 8.85 Hz, 1H), 7.37 (d, J = 8.24 Hz, 2H), 7.30 (d, J = 8.54 Hz, 2H), 6.40 (dd, J = 8.85, 2.14 Hz, 1H), 6.26 (d, J = 2.44 Hz, 1H), 4.33 (s, 2H).

4-(4-(4-Chlorophenyl)-3-(trifluoromethyl)isoxazol-5-yl)benzene-1,3-diol **4**: To a solution of 2-(4-chlorophenyl)-1-(2,4-dihydroxyphenyl)ethan-1-one **3** (1.7 g, 6.47 mmol) in pyridine (5 mL), trifluoroacetic anhydride (2.8 mL, 19.42 mmol) was added dropwise with cooling in an ice bath, and then the mixture was stirred at room temperature for 48 hours. The mixture was concentrated to dryness to yield 3-(4-chlorophenyl)-7-hydroxy-2-(trifluoromethyl)-4H-chromen-4-one, which was used for the next step. A mixture of 3-(4-chlorophenyl)-7-hydroxy-2-(trifluoromethyl)-4H-chromen-4-one and hydroxylamine hydrochloride (856.7 mg, 12.33 mmol) dissolved in pyridine was heated at

Downloaded from molpharm.aspetjournals.org at ASPET Journals on April 20, 2024

Molecular Pharmacology Fast Forward. Published on December 2, 2020 as DOI: 10.1124/molpharm.120.000106
This article has not been copyedited and formatted. The final version may differ from this version.

reflux for 12 hours and then cooled to room temperature. The reaction mixture was acidified with dilute HCl and extracted with EtOAc. The organic layer was separated and washed with saline solution, dried over anhydrous Na_2SO_4, and concentrated *in vacuo*. The resulting residue was purified by column chromatography to provide 4-(4-(4-chlorophenyl)-3-(trifluoromethyl)isoxazol-5-yl)benzene-1,3-diol **4** (800 mg, 51% yield over two steps). Characterization of **4**: ^{1}H NMR (DMSO-d_6) δ 9.96 (s, 1H), 9.95 (s,1H), 7.52-7.42 (m, 2H), 7.28 (d, J = 8.24 Hz, 2H), 7.10 (d, J = 8.24 Hz, 1H), 6.33 (d, J = 2.14 Hz, 1H), 6.28 (dd, J = 8.54, 2.14 Hz, 1H); LC-MS (m/z): 356.1 (M+H).

Fluorescence Assay and Data Analysis. Modified human embryonic kidney cells (AD-293 cells), which express stably a mutant BK_{Ca} channel (G803D/N806K) (Lee et al., 2013), were used for the cell-based assay. Cells were grown in high glucose Dulbecco's modified Eagle's medium (Hyclone, Logan, UT) containing 10% fetal bovine serum (Hyclone) and 1 mg/mL geneticin (Gibco/Life Technologies, Waltham, MA). Approximately 20,000 cells/well were seeded on a 96-well clear-bottom black-wall assay plate (Corning Incorporated, Corning, NY) coated with poly-d-lysine (Sigma-Aldrich, St. Louis, MO). The cell-based assay used a FluxOR potassium channel assay kit (Invitrogen, Eugene, OR) and was performed using the following steps. First, cell growth medium was removed, and 80 μL loading buffer containing FluxOR fluorescent dye was added to each well. The plate was then incubated at room temperature in the dark for 1 hour. After incubation, loading buffer was removed, and 100 μL assay buffer, containing varying concentrations of test compounds, was added to each well of the plate. The plate was incubated at room temperature for 20–30 min. DMSO (1 %) was used as the vehicle. 1 % of DMSO didn't affect fluorescence signal significantly. Fluorescence was measured using a FlexStation 3 multimode microplate reader (Molecular Devices, Sunnyvale, CA) and SoftMax Pro software. A hybrid multimode microplate reader (Synergy H1, BioTek Instrument Inc., Winooski, VT) and Gen5 software were used for supplemental data. The fluorescence excitation wavelength was 485 nm and the emission wavelength was 528 nm. The fluorescence signal was measured every 2 seconds for FlexStation 3 and every 10 seconds for Synergy H1. Depolarization of the cell membrane was induced chemically by addition of 20 μL stimulus buffer containing a high concentration of TI^+ to each well. For Flexstation 3, stimulus buffer

Downloaded from molpharm.aspetjournals.org at ASPET Journals on April 20, 2024

Molecular Pharmacology Fast Forward. Published on December 2, 2020 as DOI: 10.1124/molpharm.120.000106
This article has not been copyedited and formatted. The final version may differ from this version.

is added automatically 20 seconds after initiation of fluorescence measurements. In the case of Synergy H1, stimulus buffer is added manually 40 seconds after initiation of fluorescence measurements. Fluorescence signals were analyzed as relative fluorescence units (RFU or F/F_0, F_0: minimum value of fluorescence signals of each well). One-way ANOVA was used for statistical analysis. (* *P*-value < 0.05, ** *P*-value < 0.01, *** *P*-value < 0.001.)

Functional Expression of the BK_{Ca} Channel in *Xenopus* Oocytes. Rat BK_{Ca} channel α (Slo1), β1 and β4 subunits were expressed in *Xenopus laevis* oocytes for electrophysiological recording. An oocyte expression vector (pNBC1.0 or pNBC2.0) was used for rat BK_{Ca} channel subcloning and functional expression, which were carried out according to previously described methods (Ha et al., 2006). The cDNA sequence information is listed in GenBank. Accession number of the rat BK_{Ca} channel α-subunit was AF135265, β1 subunit was FJ154955.1 and β4 subunit was AY028605.

Oocytes were taken surgically from the ovarian lobes of *X. laevis* at stages V–VI (Nasco, Fort Atkinson, WI), placed in Ca^{2+}-free oocyte Ringer's (OR) culture medium (86 mM NaCl, 1.5 mM KCl, 2 mM $MgCl_2$, and 10 mM HEPES, pH 7.6) containing 3 mg/mL collagenase (Worthington Biochemicals, Freehold, NJ), and incubated for 1.5–2 hours at room temperature to remove the follicular cell layer. After incubation, oocytes were rinsed with Ca^{2+}-free OR medium and then ND-96 medium (96 mM NaCl, 2 mM KCl, 1.8 mM $CaCl_2$, 1 mM $MgCl_2$, 5 mM HEPES, and 50 g/mL gentamicin, pH 7.6). Rinsed oocytes were incubated in ND-96 medium at 18 ℃ for at least 24 hours to stabilize. Approximately 50 ng of synthesized Slo1 cRNA prepared in nuclease-free water was injected into each oocyte, after which they were incubated at 18 ℃ for 1–3 days in ND-96 medium. For the coexpression experiments, cRNA of rβ1 and rβ4 subunit were injected to each oocytes with Slo1 cRNA. Molar ratio of β subunit cRNA versus Slo1 cRNA was 12:1. That ratio guarantees sufficient coassemble of α and β subunit of BK_{Ca} channel. The vitelline membrane was removed using fine forceps before electrophysiological recordings.

Electrophysiological Recordings and Data Analysis. A giga-ohm seal patch-clamp method with membranes in an outside-out configuration was used for recording macroscopic currents, as described

Downloaded from molpharm.aspetjournals.org at ASPET Journals on April 20, 2024

Molecular Pharmacology Fast Forward. Published on December 2, 2020 as DOI: 10.1124/molpharm.120.000106
This article has not been copyedited and formatted. The final version may differ from this version.

previously (Ha et al., 2006). Borosilicate glass-pipettes (WPI, Sarasota, FL) were pulled and fire-polished, and had a resistance of 3–5 MΩ. To facilitate electrophysiological recordings, the channel current was amplified using an Axopatch 200B amplifier (Molecular Devices, San Jose, CA) and low-pass filtered at 1 kHz using a four-pole Bessel filter. The channel currents were digitized at a rate of 10 or 20 points/ms using a Digidata 1200A (Molecular Devices).

For the recording of currents, BK_{Ca} channel currents were activated by voltage-clamp pulses from -80 to 200 mV in 10 mV increments. The resting potential was held at -100 mV. Oocytes were placed in recording solution, which contained 120 mM potassium gluconate, 10 mM HEPES, 4 mM KCl, and 5 mM EGTA, pH 7.2. The MaxChelator program (Patton et al., 2004) was used to calculate the concentration of free Ca^{2+} in the intracellular solution. Intracellular solution contained 116 mM KOH, 10 mM HEPES and 4 mM KCl, pH 7. Concentration of HEDTA, EGTA and free Ca^{2+} are calculated by MaxChelator program. Solution exchange was completed within 0.5 seconds. Clampex 8.0 and Origin 9.1 software (OriginLab Corporation, Northampton, MA) were used for data acquisition and analysis. Data were summarized as mean ± SD (standard deviation). Two-tailed paired t-test was used for statistical analysis. (* *P*-value < 0.05, ** *P*-value < 0.01, *** *P*-value < 0.001.)

Isometric Tension Recording from UBSM. Experiments recording the isometric tension of UBSM were performed according to a previously described method (Lee et al. Mol Pharmacol. 2016). Briefly, bladder strips were isolated from male Sprague–Dawley rats (300–350 g). The isolated strips (approximately 2 × 8 mm) were mounted in 10 mL organ baths containing Krebs solution (118.4 mM NaCl, 4.7 mM KCl, 1.2 mM KH_2PO_4, 1.2 mM $MgSO_4$, 25.0 mM $NaHCO_3$, 2.5 mM $CaCl_2$, and 12.2 mM glucose, pH 7.4, bubbled with a mixture 95 % O_2 and 5 % CO_2 at 37°C). Isometric force measurements were recorded using a Power Lab Data Acquisition System (ADInstruments, Australia, NSW) attached to a computer installed with LabChart Software (version 7, ADInstruments). Before each experiment, bladder strips were subjected to 1 g of resting tension and allowed to equilibrate for at least 1 hour. After this equilibration period, each strip was repeatedly exposed to 10 μM ACh until constant responses were recorded with a washout period of 30 min. The strips were then pre-treated

Downloaded from molpharm.aspetjournals.org at ASPET Journals on April 20, 2024

Molecular Pharmacology Fast Forward. Published on December 2, 2020 as DOI: 10.1124/molpharm.120.000106
This article has not been copyedited and formatted. The final version may differ from this version.

for 30 min with CTIBD or 0.1% DMSO, and then ACh-induced contractile responses were measured in the presence of CTIBD or DMSO. The relaxant response to CTIBD was expressed as the percentage decrease in the ACh-induced contractile tension in the presence of CTIBD. One-way ANOVA was used for statistical analysis. (* *P*-value < 0.05, ** *P*-value < 0.01, *** *P*-value < 0.001.)

***In Vivo* Cystometry.** Adult female Sprague–Dawley rats, weighing 296 ± 15 g (approximately 13–14 weeks old) were anesthetized with isoflurane (3 %, 3 mL/min), and a polyethylene catheter (PE-50) was implanted into the bladder. Cystometry was performed 3 days after catheter insertion under anesthesia (urethane 1.3 g/kg, s.c.). The anesthetized animal was fixed supine on a vertically positioned table, so that the urethra meatus of the animal pointed downward. A plastic cup, placed underneath the urethra meatus and connected to a force transducer for weight measurement (FT0314618, Natus), was used to measure voided urine. The temperature of each animal was maintained at 37 °C during anesthesia using a heating pad. In all experiments, the bladder was first filled with saline and then infused with saline for 1 hour at room temperature at a rate of 0.05 mL/min. Then, 0.5 % acetic acids (AA) was infused to same rat until a voiding contraction occurred or for a maximum duration of 20 min, whichever happened first. CTIBD was administered intraperitoneally to same rat at a single dose of 20 mg/kg 40 min after AA administration. Intravesical pressure was recorded for 90 min after AA administration. Baseline pressure (mmHg) in the bladder, maximum pressure of voiding contraction (mmHg), inter-contraction interval (seconds), and voiding volume (mL) were averaged for a 30–90 min period post-administration in each animal. Normal saline filling, 0.5% AA infusing and intraperitoneal injection of CTIBD continuously performed at same rat. Voiding volume was measured accumulatively during experiment. One-way ANOVA was used for statistical analysis. (* *P*-value < 0.05, ** *P*-value < 0.01, *** *P*-value < 0.001.)

Animal Use Approval. This study was reviewed and approved by the Institutional Animal Care and Use Committee (IACUC) of Samsung Medical Center (SMC). SMC is and Association for Assessment and Accreditation of Laboratory Animal Care International (AAALAC International) accredited facility and abide by the Institute of Laboratory Animal Resources (ILAR) guide.

Downloaded from molpharm.aspetjournals.org at ASPET Journals on April 20, 2024

Molecular Pharmacology Fast Forward. Published on December 2, 2020 as DOI: 10.1124/molpharm.120.000106
This article has not been copyedited and formatted. The final version may differ from this version.

Downloaded from molpharm.aspetjournals.org at ASPET Journals on April 20, 2024

Molecular Pharmacology Fast Forward. Published on December 2, 2020 as DOI: 10.1124/molpharm.120.000106
This article has not been copyedited and formatted. The final version may differ from this version.

Results

Identifying BK_{Ca} Channel Activators Using a Cell-based Fluorescence Assay. A chemical library containing 8,364 chemical compounds was screened using a cell-based fluorescence assay to identify novel BK_{Ca} channel activators. One compound (Compound 1, at 5 μM) increased the fluorescence signal by almost 6-fold within 100 seconds compared with vehicle (1% DMSO) (Fig. 1A). Since Compound 1 was identified as 4-(4-phenyl)-3-(trifluoromethyl)isoxazol-5-yl)benzene-1,3-diol, we purchased other derivatives containing a 4-phenyl-isoxazol-5-yl benzene skeleton and tested their effects on the BK_{Ca} channel using the cell-based fluorescence assay. Among 19 additional compounds tested at 5 μM, 8 compounds significantly increased fluorescence at 100 seconds (Suppl. Fig. 2) with Compound 4 (or CTIBD) evoking the highest (Fig. 2B, Suppl. Fig. 2). At 5 μM, CTIBD-induced fluorescence was 7.9-fold higher than vehicle-induced fluorescence (Fig. 2C). The increase in fluorescence induced by CTIBD was concentration-dependent and blocked completely by 1 μM paxilline (Fig. 3A), a selective blocker of the BK_{Ca} channel (Sanchez and McManus, 1996). At 10 μM, CTIBD showed significant higher fluorescence levels of fluorescence compared with 3 other known BK_{Ca} activators, NS 1619, NS 11021 and Rottlerin (Suppl. Fig. 4).

Effects of CTIBD on the Macroscopic Currents of the BK_{Ca} Channel. To validate the cell-based assay results, we determined the effects of CTIBD on the BK_{Ca} channel using electrophysiology. The α-subunit of the wild-type rat BK_{Ca} channel was expressed in *Xenopus* oocytes, and the macroscopic current of excised oocyte membranes was measured. The excised membrane configuration was outside-out, and the intracellular Ca^{2+} concentration was fixed at 3 μM. CTIBD was applied to the extracellular side of the excised membrane at 3 μM, 30 seconds after initiation of current measurements (Fig. 4). CTIBD increased the amplitude of macroscopic currents in a time-dependent manner (Fig. 4b and c) from basal level (Fig. 4a). After removal of CTIBD, the channel currents decreased almost completely to basal level (Fig. 4d). CTIBD appeared to mediate the potentiation and depotentiation process of the BK_{Ca} channel in two phases. During the potentiation process, for example, the channel current increased rapidly within a few seconds, and then increased more steadily

Downloaded from molpharm.aspetjournals.org at ASPET Journals on April 20, 2024

Molecular Pharmacology Fast Forward. Published on December 2, 2020 as DOI: 10.1124/molpharm.120.000106
This article has not been copyedited and formatted. The final version may differ from this version.

and gradually over a few minutes. Thus, the current data were fitted with a double-exponential function, and the time-constants were estimated as 5.1 ± 2.6 and 48.3 ± 8.8 seconds for association, and 4.3 ± 3.1 and 76.1 ± 32.0 seconds for dissociation.

We then investigated the mechanism of CTIBD-induced BK_{Ca} channel potentiation. A series of voltage pulses were applied to activate the BK_{Ca} channel, and macroscopic currents were measured under different concentrations of CTIBD. When the extracellular concentration of CTIBD was increased, the channel was activated at a lower voltage, and the tail currents evoked by repolarization were drastically increased (Fig. 5A). Fig. 5B represents the conductance–voltage (*G–V*) relationship of BK_{Ca} channel macroscopic currents under varying concentrations of CTIBD. Application of CTIBD shifted the *G–V* curve to a more negative voltage and increased the maximum conductance (G_{max}) in a concentration-dependent manner. The concentration-dependent shift of the *G–V* relationship was quantified in terms of half-activation voltage ($V_{1/2}$), shown in Fig. 5C. As the extracellular concentration of CTIBD was increased from 0.1 to 10 μM, $V_{1/2}$ decreased by approximately 50 mV from 155.8 ± 5.8 to 105.7 ± 4.4 mV. These results indicate that CTIBD lowers the threshold voltage for activation and increases the maximum open probability of the BK_{Ca} channel. A large negative shift of *G-V* relationship by CTIBD was also observed at basal intracellular Ca^{2+} concentration of 0.1 μM (Suppl. Fig. 5).

Effects of CTIBD on Gating Kinetics of the BK_{Ca} Channel. Since the tail currents of the BK_{Ca} channel were increased by CTIBD (Fig. 5A), we further investigated the effects of this compound on gating kinetics. Fig. 6 shows the activation and deactivation kinetics of the BK_{Ca} channel when analyzed in the absence and presence of 10 μM CTIBD. Fig. 6A and 6B show representative current traces of activation (or opening) and deactivation (or closing), respectively, of the BK_{Ca} channel in the presence of 10 μM compound. The activation time-constant ($\tau_{activation}$) values were obtained by fitting the current traces using a single-exponential function at each voltage (Fig. 6C). In the presence of 10 μM CTIBD, the activation rate was slightly increased at all voltages tested. The effects of CTIBD on channel deactivation were dramatic, and the deactivation time-constant ($\tau_{deactivation}$) greatly increased

Downloaded from molpharm.aspetjournals.org at ASPET Journals on April 20, 2024

Molecular Pharmacology Fast Forward. Published on December 2, 2020 as DOI: 10.1124/molpharm.120.000106
This article has not been copyedited and formatted. The final version may differ from this version.

(Fig. 6D). Channel closing greatly slowed in the presence of 10 μM CTIBD at all voltages tested. The deactivation rate decreased by 11.5-fold at 160 mV in the presence of 10 μM CTIBD. These results indicate that CTIBD potentiates BK_{Ca} channel activity by slowing channel closing with minimal effects on channel opening, and suggest that upon binding to the channel, the compound stabilizes the activation conformation of the BK_{Ca} channel.

Effects of β Subunits on CTIBD-induced Activation of the BK_{Ca} Channel. Functional characteristics of BK_{Ca} channel is altered by auxiliary β subunits. The effects of channel modulators also can be affected by the presence of β subunits. In Fig. 7 and Fig. 8, the effect of β subunits on CTIBD-induced potentiation of BK_{Ca} channel was examined. cRNA of rSlo and rat β subunits were injected together to express rSlo/rβ1 or rSlo/rβ4 heteromeric BK_{Ca} channels. Vehicle (0.1 % DMSO) or 10 μM CTIBD were treated to the extracellular side of membrane. At 10 μM CTIBD, rSlo/rβ1 channel show slight but significant shift of *G-V* relationship. $V_{1/2}$ values of vehicle treated channel and 10 μM CTIBD treated channel were 114.9 ± 6.7 mV and 98.1 ± 8.1 mV, respectively (Fig. 7B). In the case of rSlo/rβ4 channel, $V_{1/2}$ value was decreased approximately 40 mV from 163.5 ± 13.9 mV to 121.5 ± 8.4 mV at 10 μM CTIBD (Fig. 8B).

Activation and deactivation time constant were also analyzed in Fig. 7 and Fig. 8. Activation time constant of rSlo/rβ1 coexpressed BK_{Ca} channel was slightly increased by CTIBD but did not show significant difference compared with vehicle treated condition (Fig. 7C). On the other hand, deactivation time constant of rSlo/rβ1 coexpressed BK_{Ca} channel was increased by CTIBD significantly (Fig. 7D). In the case of rSlo/rβ4 coexpressed BK_{Ca} channel, activation time constant was slightly decreased by CTIBD, but it was only significant at low voltage pulses between 150 to 170 mV (Fig. 8C). Deactivation time constant of rSlo/rβ4 coexpressed BK_{Ca} channel was dramatically increased by CTIBD (Fig. 8D). The deactivation rate decreased by 7.6-fold at 150 mV in the presence of 10 μM CTIBD. These results indicate that CTIBD activates both rSlo/rβ1 and rSlo/rβ4 channels

Downloaded from molpharm.aspetjournals.org at ASPET Journals on April 20, 2024

Molecular Pharmacology Fast Forward. Published on December 2, 2020 as DOI: 10.1124/molpharm.120.000106
This article has not been copyedited and formatted. The final version may differ from this version.

mainly by decreasing the closing rate of the channel same as rSlo homomeric channel but with much less extent.

Relaxation Effect of CTIBD on Rat Bladder Smooth Muscle Strips. Since it is well documented that the activation of the BK_{Ca} channel relaxes the smooth muscle in the bladder, we investigated whether CTIBD exerted relaxation effects on excised bladder strips from rats (Fig. 9). Initially, 10 μM acetylcholine (ACh) was applied to rat detrusor muscle strips, and the isometric tension was measured. ACh treatment caused the tension to rise dramatically. Immediately afterward, tension decreased and plateaued at half of the peak level. Pretreatment with CTIBD concentration-dependently reduced ACh-induced peak contractions (Fig. 9A). Although 3 and 10 μM CTIBD did not produce a significant relaxation, significant relaxations by CTIBD were observed at higher concentrations: 42.1 ± 21.1 % at 30 μM, 65.3 ± 14.0 % at 100 μM, and 81.4 ± 10.2 % at 300 μM compared with controls (Fig. 9B). EC_{50} value of CTIBD was determined as 28.0 ± 5.0 μM. CTIBD did not show any relaxation effect on rat bladder strips at basal condition without ACh (Suppl. Fig.6).

Effects of CTIBD on the Micturition Function of OAB Rats. To observe the therapeutic effects of CTIBD on micturition, CTIBD was injected intraperitoneally into an AA-induced rat model of OAB. Rats infused with normal saline showed three voiding contractions at regular intervals, whereas rats treated with 0.5 % AA showed hyperactive frequent voiding contractions (Fig. 10A, middle panel). Pretreatment of rats with 20 mg/kg CTIBD decreased the number of voiding contractions to basal levels (Fig. 10A, right panel). Thus, CTIBD restored the frequency of AA-induced voiding contractions to the basal state. During the *in vivo* cystometry experiments, basal pressure, maximum pressure of voiding contraction, inter-contraction interval, and voiding volume were analyzed (Fig. 10B). CTIBD treatment did not significantly alter basal pressure or maximum pressure of voiding contraction. However, CTIBD treatment increased 0.5 % AA-induced decreases in the inter-contraction interval (Fig. 10D) and voiding volume significantly (Fig. 10E). These results indicate that CTIBD produces anti-OAB effects in rats, most likely caused by relaxation of bladder detrusor muscle.

Downloaded from molpharm.aspetjournals.org at ASPET Journals on April 20, 2024

Molecular Pharmacology Fast Forward. Published on December 2, 2020 as DOI: 10.1124/molpharm.120.000106
This article has not been copyedited and formatted. The final version may differ from this version.

Downloaded from molpharm.aspetjournals.org at ASPET Journals on April 20, 2024

Molecular Pharmacology Fast Forward. Published on December 2, 2020 as DOI: 10.1124/molpharm.120.000106
This article has not been copyedited and formatted. The final version may differ from this version.

Discussion

In this study, we aimed to identify new chemical activators of the BK_{Ca} channel that contained novel skeletons. Initially, a chemical library containing 8,364 unique compounds was screened using a cell-based fluorescence assay that we previously established (Lee et al., 2013). From the library, 25 compounds evoked a fluorescence that was at least 1.5-fold higher than vehicle (1% DMSO) at 100 milliseconds (*data not shown*). A single compound, identified subsequently as 4-(4-phenyl)-3-(trifluoromethyl)isoxazol-5-yl)benzene-1,3-diol (compound 1), was prominent in rapidly and robustly increasing fluorescence (Fig. 1). We then purchased 19 additional compounds containing a phenyl-isoxazolyl benzene skeleton for a structure–activity relationship (SAR) study.

Among the 20 compounds tested, 9 compounds increased fluorescence significantly with *P*-values < 0.05 (Fig. 2, Suppl. Fig. 2). Three compounds were especially potent in the fluorescence assay. EC_{50} values were determined as 7.7 ± 0.5 μM for Compound 1, 3.9 ± 0.6 μM for Compound 4, and 9.4 ± 1.7 μM for Compound 7. Thus, Compound 4 (CTIBD) was chosen for further study (Suppl. Fig. 3). Compound 4 (CTIBD) increased the fluorescence signal most rapidly and highly among all derivatives tested in a concentration-dependent manner (Fig. 3). Results from the SAR study suggest that m-dihydroxy and CF_3 moieties are essential for activity as channel activators. Although compound 4, with a p-chloro substituent of (4-(4-(4-chlorophenyl)-3-(trifluoromethyl)isoxazol-5-yl)benzene-1,3-diol), was most active, there is clearly room for further optimization of this class of compounds, and thus more extensive SAR studies would be of great value.

We validated the potentiating effects of CTIBD on BK_{Ca} channel activity and investigated its mechanism of action. Application of CTIBD to the extracellular side of the channel reversibly and concentration-dependently potentiated macroscopic currents of the BK_{Ca} channel (Fig. 4). The potentiation and de-potentiation trajectories could be fitted with double-exponential functions, indicating that the channel current comprised two different phases: an early fast phase and a late slow

Downloaded from molpharm.aspetjournals.org at ASPET Journals on April 20, 2024

Molecular Pharmacology Fast Forward. Published on December 2, 2020 as DOI: 10.1124/molpharm.120.000106
This article has not been copyedited and formatted. The final version may differ from this version.

phase. One plausible explanation for this is that CTIBD simply has two different binding sites on the channel, each with distinct affinities: one site with high affinity and the other with lower affinity. Since the BK_{Ca} channel is composed of four α-subunits, four identical affinity sites should exist in a tetrameric holo-channel with 4-fold symmetry. Thus, it is also conceivable in that the binding of CTIBD to a single site of high affinity may convert another site to a lower affinity binding site. It will be intriguing to determine experimentally the stoichiometry of CTIBD binding to individual channel subunits, and also to determine the binding site on the channel that is responsible for current potentiation.

Mechanistically, CTIBD affects both voltage-dependent activation and maximum conductance of the channel. CTIBD concentration-dependently shifted the *G–V* relationship of the BK_{Ca} channel progressively to a negative direction (Fig. 5). Based on extrapolation, the maximum shift of $V_{1/2}$ value was estimated as -70.3 mV. CTIBD also increases the maximum channel conductance at a given voltage. It is reported that the open probability of the BK_{Ca} channel does not reach unity even at extreme positive voltages (Ma et al., 2006; Sigg and Bezanilla, 1997). It will be intriguing to reveal in future research the mechanism of how the binding of CTIBD increases the maximum open probability and thus the maximum conductance of the BK_{Ca} channel. Kinetically, CTIBD potentiated the activity of the BK_{Ca} channel by dramatically slowing channel closing without significantly affecting the activation rate. At 10 μM CTIBD, the closing rate of the channel was slowed by 11.6-fold at 160 mV. It is likely that CTIBD binds to the open conformation of the channel more tightly, thus stabilizing the open state of the channel and preventing the channel from closing.

Since the functional characteristics are altered by auxiliary β subunits, the effects of β subunits on CTIBD-induced BK_{Ca} channel activation were studied. Two main β subunits, β1 and β4 subunits, were expressed together with α (or Slo). It is worth mentioning that these two β subunits are known to express predominantly in the bladder (Petkov, 2014; Poulsen et al., 2009). CTIBD shifted the *G-V* curve of both rSlo/rβ1 and rSlo/rβ4 channels to negative direction (Fig. 7, Fig. 8). While 10 μM CTIBD shifted the $V_{1/2}$ value of rSlo/rβ1 approximately -16 mV, the same concentration of

Downloaded from molpharm.aspetjournals.org at ASPET Journals on April 20, 2024

Molecular Pharmacology Fast Forward. Published on December 2, 2020 as DOI: 10.1124/molpharm.120.000106
This article has not been copyedited and formatted. The final version may differ from this version.

CTIBD shifted the $V_{1/2}$ of rSlo/rβ4 channel as much as -40 mV. Thus, the potentiation of BK_{Ca} channel by CTIBD was decreased by coexpression of both β1 and β4 subunits, but the reduced activation was more significant for β1 than β4. The expression of β subunits also affected differentially the gating kinetics of CTIBD-induced BK_{Ca} channel activation and deactivation. CTIBD activates both rSlo/rβ1 and rSlo/rβ4 channels mainly by slowing down the channel closure. A similar kinetic effects of CTBID was also observed for the homomeric Slo channel but with more significant without β subunits.

The BK_{Ca} channel plays an important role in the contraction of UBSM by controlling the resting membrane potential and repolarization phase. Thus, we tested the effect of CTIBD on the relaxation of excised rat UBSM strips. As expected, pretreatment with CTIBD concentration-dependently inhibited ACh-induced contraction of rat UBSM strips at 30 μM or higher concentrations. At the highest concentration of 300 μM, CTIBD inhibited ACh-induced contraction by 81.4 % compared with negative control. These results indicate that CTIBD relaxes UBSM. We then tested the efficacy of CTIBD on micturition in a rat model of AA-evoked OAB. Acetic acids enhance sensitivity of neuronal activity of bladder smooth muscle cell and it causes OAB on rat model (Choudhary et al., 2015; Mitobe et al., 2008). Using *in vivo* cystometry, intraperitoneal injection of CTIBD (20 mg/kg) relaxed AA-induced frequent voiding contraction significantly. It is worth noting and encouraging that other parameters of bladder functions, such as the basal intravesical pressure and the maximum pressure of voiding contraction, were not significantly affected by CTIBD treatment.

In summary, a series of new BK_{Ca} channel activators containing a 4-phenyl-isoxazol-5-yl benzene skeleton were identified, and one compound (CTIBD) was characterized as a novel potent activator of the channel. CTIBD potentiated the activity of the channel by directly binding to the channel and stabilizing its open conformation. In rats, CTIBD effectively relaxes UBSM *ex vivo* and bladder hyperactivity *in vivo*. Taken together, these results indicate that CTIBD and its derivatives that target the bladder BK_{Ca} channel can be considered as strong new candidates for OAB therapeutics.

Downloaded from molpharm.aspetjournals.org at ASPET Journals on April 20, 2024

Molecular Pharmacology Fast Forward. Published on December 2, 2020 as DOI: 10.1124/molpharm.120.000106
This article has not been copyedited and formatted. The final version may differ from this version.

Acknowledgements

The chemical library used in this study was kindly provided by the Korea Chemical Bank (www.chembank.org) of the Korea Research Institute of Chemical Technology.

Downloaded from molpharm.aspetjournals.org at ASPET Journals on April 20, 2024

Molecular Pharmacology Fast Forward. Published on December 2, 2020 as DOI: 10.1124/molpharm.120.000106
This article has not been copyedited and formatted. The final version may differ from this version.

Authorship Contributions

Participated in research design: N. Lee, Park.

Conducted experiments: N. Lee, Lim, K. S. Lee, Shin, S. W. Lee, Kang.

Contributed new reagents or analytic tools: H. S. Pagire, S. H. Pagire, Ahn.

Performed data analysis: N. Lee, Lim, K. S. Lee, Shin, S. W. Lee, Kang, Park

Wrote or contributed to the writing of the manuscript: N. Lee, S. W. Lee, Kang, Ahn, Park.

Downloaded from molpharm.aspetjournals.org at ASPET Journals on April 20, 2024

Molecular Pharmacology Fast Forward. Published on December 2, 2020 as DOI: 10.1124/molpharm.120.000106
This article has not been copyedited and formatted. The final version may differ from this version.

References

Abrams P and Andersson KE (2007) Muscarinic receptor antagonists for overactive bladder. *BJU international* **100**(5): 987-1006.

Barrett J, Magleby K and Pallotta B (1982) Properties of single calcium-activated potassium channels in cultured rat muscle. *The Journal of Physiology* **331**(1): 211-230.

Bo X and Burnstock G (1990) The effects of Bay K 8644 and nifedipine on the responses of rat urinary bladder to electrical field stimulation, beta, gamma-methylene ATP and acetylcholine. *British journal of pharmacology* **101**(2): 494.

Cerruto M, Asimakopoulos A, Artibani W, Del Popolo G, La Martina M, Carone R and Finazzi-Agrò E (2012) Insight into new potential targets for the treatment of overactive bladder and detrusor overactivity. *Urologia internationalis* **89**(1): 1-8.

Choudhary M, van Asselt E, van Mastrigt R and Clavica F (2015) Neurophysiological modeling of bladder afferent activity in the rat overactive bladder model. *The Journal of Physiological Sciences* **65**(4): 329-338.

Cui J, Yang H and Lee US (2009) Molecular mechanisms of BK channel activation. *Cellular and Molecular Life Sciences* **66**(5): 852-875.

Du W, Bautista JF, Yang H, Diez-Sampedro A, You S-A, Wang L, Kotagal P, Lüders HO, Shi J and Cui J (2005) Calcium-sensitive potassium channelopathy in human epilepsy and paroxysmal movement disorder. *Nature genetics* **37**(7): 733-738.

Eglen RM, Choppin A, Dillon MP and Hegde S (1999) Muscarinic receptor ligands and their therapeutic potential. *Current opinion in chemical biology* **3**(4): 426-432.

Gribkoff VK, Starrett Jr JE and Dworetzky SI (2001) Maxi-K potassium channels: form, function, and modulation of a class of endogenous regulators of intracellular calcium. *The Neuroscientist* **7**(2): 166-177.

Ha TS, Lim H-H, Lee GE, Kim Y-C and Park C-S (2006) Electrophysiological characterization of benzofuroindole-induced potentiation of large-conductance Ca2+-activated K+ channels. *Molecular pharmacology* **69**(3): 1007-1014.

Hegde SS and Eglen RM (1999) Muscarinic receptor subtypes modulating smooth muscle contractility in the urinary bladder. *Life sciences* **64**(6-7): 419-428.

Hristov KL, Chen M, Kellett WF, Rovner ES and Petkov GV (2011) Large-conductance voltage-and Ca2+-activated K+ channels regulate human detrusor smooth muscle function. *American Journal of Physiology-Cell Physiology* **301**(4): C903-C912.

Kay GG and Granville LJ (2005) Antimuscarinic agents: Implications and concerns in themanagement of overactive bladder in the elderly. *Clinical therapeutics* **27**(1): 127-138.

Layne JJ, Nausch B, Olesen S-P and Nelson MT (2010) BK channel activation by NS11021 decreases excitability and contractility of urinary bladder smooth muscle. *American Journal of Physiology-Regulatory, Integrative and Comparative Physiology* **298**(2): R378-R384.

Lee B-C, Kim H-J, Park SH, Phuong TTT, Kang TM and Park C-S (2013) Development of cell-based assay system that utilizes a hyperactive channel mutant for high-throughput screening of BKCa channel modulators. *Journal of biotechnology* **167**(1): 41-46.

Ma Z, Lou XJ and Horrigan FT (2006) Role of charged residues in the S1–S4 voltage sensor of BK channels. *The Journal of general physiology* **127**(3): 309-328.

Marty A (1981) Ca-dependent K channels with large unitary conductance in chromaffin cell membranes. *Nature* **291**(5815): 497-500.

Meredith AL, Wiler SW, Miller BH, Takahashi JS, Fodor AA, Ruby NF and Aldrich RW (2006) BK calcium-activated potassium channels regulate circadian behavioral rhythms and pacemaker output. *Nature neuroscience* **9**(8): 1041-1049.

Mitobe M, Inoue H, Westfall TD, Higashiyama H, Mizuyachi K, Kushida H and Kinoshita M (2008) A new method for producing urinary bladder hyperactivity using a non-invasive transient intravesical infusion of acetic acid in conscious rats. *Journal of pharmacological and toxicological methods* **57**(3): 188-193.

Orio P, Rojas P, Ferreira G and Latorre R (2002) New disguises for an old channel: MaxiK channel β-subunits. *Physiology* **17**(4): 156-161.

Patton C, Thompson S and Epel D (2004) Some precautions in using chelators to buffer metals in biological solutions. *Cell calcium* **35**(5): 427-431.

Petkov GV (2014) Central role of the BK channel in urinary bladder smooth muscle physiology and pathophysiology. *American Journal of Physiology-Regulatory, Integrative and Comparative Physiology* **307**(6): R571-R584.

Downloaded from molpharm.aspetjournals.org at ASPET Journals on April 20, 2024

Molecular Pharmacology Fast Forward. Published on December 2, 2020 as DOI: 10.1124/molpharm.120.000106
This article has not been copyedited and formatted. The final version may differ from this version.

Poulsen AN, Wulf H, Hay-Schmidt A, Jansen-Olesen I, Olesen J and Klaerke DA (2009) Differential expression of BK channel isoforms and β-subunits in rat neuro-vascular tissues. *Biochimica et Biophysica Acta (BBA)-Biomembranes* **1788**(2): 380-389.

Salkoff L, Butler A, Ferreira G, Santi C and Wei A (2006) High-conductance potassium channels of the SLO family. *Nature Reviews Neuroscience* **7**(12): 921-931.

Sanchez M and McManus O (1996) Paxilline inhibition of the alpha-subunit of the high-conductance calcium-activated potassium channel. *Neuropharmacology* **35**(7): 963-968.

Sigg D and Bezanilla F (1997) Total charge movement per channel: the relation between gating charge displacement and the voltage sensitivity of activation. *The Journal of general physiology* **109**(1): 27-39.

Sprossmann F, Pankert P, Sausbier U, Wirth A, Zhou XB, Madlung J, Zhao H, Bucurenciu I, Jakob A and Lamkemeyer T (2009) Inducible knockout mutagenesis reveals compensatory mechanisms elicited by constitutive BK channel deficiency in overactive murine bladder. *The FEBS journal* **276**(6): 1680-1697.

Stewart W, Van Rooyen J, Cundiff G, Abrams P, Herzog A, Corey R, Hunt T and Wein A (2003) Prevalence and burden of overactive bladder in the United States. *World journal of urology* **20**(6): 327-336.

Wang X, Inukai T, Greer MA and Greer SE (1994) Evidence that Ca2+-activated K+ channels participate in the regulation of pituitary prolactin secretion. *Brain research* **662**(1-2): 83-87.

Wang Z-W (2008) Regulation of synaptic transmission by presynaptic CaMKII and BK channels. *Molecular neurobiology* **38**(2): 153-166.

Werner ME, Knorn A-M, Meredith AL, Aldrich RW and Nelson MT (2007) Frequency encoding of cholinergic- and purinergic-mediated signaling to mouse urinary bladder smooth muscle: modulation by BK channels. *American Journal of Physiology-Regulatory, Integrative and Comparative Physiology* **292**(1): R616-R624.

Werner ME, Zvara P, Meredith AL, Aldrich RW and Nelson MT (2005) Erectile dysfunction in mice lacking the large-conductance calcium-activated potassium (BK) channel. *The Journal of physiology* **567**(2): 545-556.

Wu RS and Marx SO (2010) The BK potassium channel in the vascular smooth muscle and kidney: α-and β-subunits. *Kidney international* **78**(10): 963-974.

Yang H, Zhang G and Cui J (2015) BK channels: multiple sensors, one activation gate. *Frontiers in physiology* **6**: 29.

Downloaded from molpharm.aspetjournals.org at ASPET Journals on April 20, 2024

Molecular Pharmacology Fast Forward. Published on December 2, 2020 as DOI: 10.1124/molpharm.120.000106
This article has not been copyedited and formatted. The final version may differ from this version.

Footnotes

This work was supported by the Korea Institute of Planning and Evaluation for Technology in Food, Agriculture, and Forestry (IPET) through the Agri-Bio Industry Technology Development Program, funded by the Ministry of Agriculture, Food and Rural Affairs (MAFRA) (317070-4) and supported by GIST Research Institute (GRI) IIBR grant funded in 2020.

Downloaded from molpharm.aspetjournals.org at ASPET Journals on April 20, 2024

Molecular Pharmacology Fast Forward. Published on December 2, 2020 as DOI: 10.1124/molpharm.120.000106
This article has not been copyedited and formatted. The final version may differ from this version.

Legends for Figures

Fig. 1. Screening of a chemical library using a cell-based fluorescence assay. A chemical library of 8,364 compounds (KRICT Diversity Library) was screened to identify novel BK_{Ca} channel activators. A hyperactive mutant BK_{Ca} channel (G803D/N806K) expressed in AD-293 cells was used for the fluorescence assay. (A) Representative fluorescence traces of eight different compounds and vehicle (1 % DMSO) are shown. Each compound was added to each well at a final concentration of 5 μM before the fluorescence signal was measured. At 20 seconds, stimulus buffer was added. Empty squares indicate vehicle (□, 1 % DMSO) and filled squares indicate Compound 1 (■). The RFU (relative fluorescent units) value (B), and fold increase in RFU normalized to vehicle (C) of eight compounds and vehicle, are shown. The RFU value and fold increase were measured at 100 seconds. The black bar indicates Compound 1. Each error bar indicates S.D (standard deviation). (n = 3)

Fig. 2. Structure–activity relationship (SAR) study of compounds related to Compound 1. A hyperactive mutant BK_{Ca} channel (G803D/N806K) expressed in AD-293 cells was used for the fluorescence assay. (A) Structures of the compounds tested in the SAR study. (B) Representative fluorescence traces of each compound, which were tested at 5 μM. Vehicle was DMSO (1 %). (C) Fold increases (obtained at 100 seconds) in the relative fluorescence units (RFU) of each tested compound normalized to DMSO are shown. Each error bar indicates S.D. One-way ANOVA followed by Dunn-Sidak's post-test was used for statistical analysis. (n = 3, * *P*-value < 0.05, ** *P*-value < 0.01, *** *P*-value < 0.001, compared with vehicle.)

Fig. 3. CTIBD concentration-dependently increased fluorescence signals. The activity of various concentrations of CTIBD (0.1 μM (■), 0.3 μM (●), 1 μM (▲), 3 μM (▼), 5 μM (◆), 10 μM (◀))

Downloaded from molpharm.aspetjournals.org at ASPET Journals on April 20, 2024

Molecular Pharmacology Fast Forward. Published on December 2, 2020 as DOI: 10.1124/molpharm.120.000106
This article has not been copyedited and formatted. The final version may differ from this version.

and vehicle (□, 1 % DMSO) were tested on a hyperactive mutant BK_{Ca} channel expressed in AD-293 cells. (A) Representative fluorescence traces are shown. Cells were treated with CTIBD prior to fluorescence measurements, and stimulus buffer was added at 20 seconds. In some wells, 5 μM CTIBD and 1 μM paxilline (⬒) was added simultaneously. (B) Fold increase in RFU normalized to vehicle (1 % DMSO) induced by different concentrations of CTIBD. Empty bar is vehicle, black bars are different concentrations of CTIBD, and striped bar is 5 μM CTIBD and 1 μM paxilline. Each error bar indicates S.D. One-way ANOVA followed by Dunn-Sidak's post-test was used for statistical analysis. (n = 4, * *P*-value < 0.05, ** *P*-value < 0.01, *** *P*-value < 0.001, compared with vehicle.)

Fig. 4. CTIBD induced a reversible potentiation of macroscopic outward currents of the BK_{Ca} channel. A representative plot of the BK_{Ca} channel outward currents is shown. BK_{Ca} channel was activated once every second by a 100 mV pulse. The duration of each voltage pulse was 50 milliseconds (ms), and the holding voltage was -100 mV. Macroscopic currents of the BK_{Ca} channel were recorded once every second. Dots on the representative plot indicate the mean value of the outward current. After initiation of 100 mV pulses, mean currents were obtained from outward current values between 20 and 40 ms. Representative current traces (a–d) show current traces of arrow pointed spots.

Fig. 5. Effects of CTIBD on the conductance–voltage relationship and $V_{1/2}$. (A) Representative current traces of the BK_{Ca} channel. Intracellular Ca^{2+} concentration was 3 μM. Vehicle was DMSO (0.1 %). Various concentrations of CTIBD were applied to the extracellular side of the channel. Duration of the voltage pulses was 100 ms. Currents were recorded at every voltage pulse, which were increased from -80 to 200 mV in 10 mV increments. The holding voltage was -100 mV. Representative current traces at every 20 mV from -80 to 200 mV are shown. (B) Effects of CTIBD on the conductance–voltage relationship of the BK_{Ca} channel. Intracellular Ca^{2+} concentration was 3μM. After initiation of voltage pulses, mean conductances were obtained from outward current values obtained between 40 and 60

Downloaded from molpharm.aspetjournals.org at ASPET Journals on April 20, 2024

Molecular Pharmacology Fast Forward. Published on December 2, 2020 as DOI: 10.1124/molpharm.120.000106
This article has not been copyedited and formatted. The final version may differ from this version.

ms. All currents were normalized to the maximum current obtained with 10 μM CTIBD. Vehicle (□, 0.1 % DMSO, n = 6) and 0.1 μM (■, n = 6), 0.3 μM (●, n = 5), 0.5 μM (▲, n = 4), 1 μM (▼, n = 4), 3 μM (◆, n = 4), or 10 μM (◀, n = 4) of CTIBD was applied to the extracellular side of the channel. (C) Effects of CTIBD on $V_{1/2}$. To obtain $V_{1/2}$, each current trace was individually fitted using the Boltzmann function, $G/G_{max} = \{(G_{max} - G_{min}) / (1 + \exp[(V_{1/2}-V) / k])\} + G_{min}$, where G = conductance. Each error bar indicates S.D.

Fig. 6. Effects of CTIBD on the activation and deactivation of the BK_{Ca} channel. Representative current traces of activation (A) and deactivation (B) are shown. Vehicle (0.1 % DMSO, gray lines) and 10 μM CTIBD (black) were added to the extracellular side of the channel. All current traces were obtained at 150 mV. (C) Activation time-constant ($\tau_{activation}$) of the vehicle (□, 0.1 % DMSO, n = 4)-treated and 10 μM CTIBD (■, n = 4)-treated BK_{Ca} channel. (D) Deactivation time-constant ($\tau_{deactivation}$) of the vehicle (□, 0.1 % DMSO, n = 4)-treated and 10 μM CTIBD (■, n = 4)-treated BK_{Ca} channel. Each error bar indicates S.D. To obtain time-constant values, all current traces were fitted individually with the exponential standard function ($y(t) = A_1\exp(-t/\tau_1) + C$) in the Clampfit program. Two-tailed paired t-test was used for statistical analysis. (* P-value < 0.05, ** P-value < 0.01, *** P-value < 0.001.)

Fig. 7. Effects of β1 subunits on CTIBD-induced activation of BK_{Ca} channel. $[Ca^{2+}]_i$ was 3μM. (A) Representative current traces of rSlo/rβ1 coexpression channel. Vehicle was DMSO (0.1 %). 10 μM of CTIBD were applied to the extracellular side of the channel. Duration of the voltage pulses was 100 ms. Currents were recorded at every voltage pulse, which were increased from -80 to 200 mV in

Downloaded from molpharm.aspetjournals.org at ASPET Journals on April 20, 2024

Molecular Pharmacology Fast Forward. Published on December 2, 2020 as DOI: 10.1124/molpharm.120.000106
This article has not been copyedited and formatted. The final version may differ from this version.

10 mV increments. The holding voltage was -100 mV. Representative current traces at every 20 mV from -80 to 200 mV are shown. (B) Effects of CTIBD on the conductance–voltage relationship of rSlo/rβ1 coexpression channel. After initiation of voltage pulses, mean conductances were obtained from outward current values obtained between 40 and 60 ms. All currents were normalized to the maximum current obtained with 10 μM CTIBD. Vehicle (□, 0.1 % DMSO, n = 3) and 10 μM (■, n = 3) of CTIBD was applied to the extracellular side of the channel. (C) Activation time-constant ($\tau_{activation}$) of the vehicle (□, 0.1 % DMSO, n = 3)-treated and 10 μM CTIBD (■, n = 3)-treated rSlo/rβ1 coexpression channel. (D) Deactivation time-constant ($\tau_{deactivation}$) of the vehicle (□, 0.1 % DMSO, n = 3)-treated and 10 μM CTIBD (■, n = 3)-treated rSlo/rβ1 coexpression channel. Each error bar indicates S.D. To obtain time-constant values, all current traces were fitted individually with the exponential standard function ($y(t) = A_1\exp(-t/\tau_1) + C$) in the Clampfit program. Two-tailed paired t-test was used for statistical analysis. (* *P*-value < 0.05, ** *P*-value < 0.01, *** *P*-value < 0.001.)

Fig. 8. Effects of β4 subunits on CTIBD-induced activation of BK_{Ca} channel. $[Ca^{2+}]_i$ was 3μM. (A) Representative current traces of rSlo/rβ4 coexpression channel. Vehicle was DMSO (0.1 %). 10 μM of CTIBD were applied to the extracellular side of the channel. Duration of the voltage pulses was 100 ms. Currents were recorded at every voltage pulse, which were increased from -80 to 200 mV in 10 mV increments. The holding voltage was -100 mV. Representative current traces at every 20 mV from -80 to 200 mV are shown. (B) Effects of CTIBD on the conductance–voltage relationship of rSlo/rβ4 coexpression channel. After initiation of voltage pulses, mean conductances were obtained from outward current values obtained between 40 and 60 ms. All currents were normalized to the maximum current obtained with 10 μM CTIBD. Vehicle (□, 0.1 % DMSO, n = 4) and 10 μM (■, n = 4) of CTIBD was applied to the extracellular side of the channel. (C) Activation time-constant

Downloaded from molpharm.aspetjournals.org at ASPET Journals on April 20, 2024

Molecular Pharmacology Fast Forward. Published on December 2, 2020 as DOI: 10.1124/molpharm.120.000106
This article has not been copyedited and formatted. The final version may differ from this version.

($\tau_{activation}$) of the vehicle (□, 0.1 % DMSO, n = 4)-treated and 10 μM CTIBD (■, n = 4)-treated rSlo/rβ4 coexpression channel. (D) Deactivation time-constant ($\tau_{deactivation}$) of the vehicle (□, 0.1 % DMSO, n = 4)-treated and 10 μM CTIBD (■, n = 4)-treated rSlo/rβ4 coexpression channel. Each error bar indicates S.D. To obtain time-constant values, all current traces were fitted individually with the exponential standard function ($y(t) = A_1\exp(-t/\tau_1) + C$) in the Clampfit program. Two-tailed paired t-test was used for statistical analysis. (* *P*-value < 0.05, ** *P*-value < 0.01, *** *P*-value < 0.001.)

Fig. 9. Effect of CTIBD on ACh-induced contractions in isolated rat urinary bladder strips. Contractions were induced by ACh (10 μM) 30 min after addition of CTIBD or control (0.1 % DMSO) (A) Representative traces of the CTIBD-induced relaxation response. (B) Percentage relaxation, expressed as the decrease in Ach-induced contraction produced by CTIBD relative to the maximum ACh-induced contraction. Each error bar indicates S.D. One-way ANOVA followed by Dunn-Sidak's post-test was used for statistical analysis. (n = 8 or 9, * *P*-value < 0.05, ** *P*-value < 0.01, *** *P*-value < 0.001, compared with control.)

Fig. 10. *In vivo* cystometry. (A) Representative traces of cystometrogram data in rats treated with normal saline, 0.5% acetic acid (to induce bladder hyperactivity), and CTIBD. In CTIBD-treated rats, 20 mg/kg CTIBD was intraperitoneally injected after 0.5 % acetic acid treatment. Basal pressure (B), maximum pressure of voiding contraction (C), inter-contraction interval (D), and voiding volume (E) of rats treated with normal saline, 0.5 % acetic acid, or 20 mg/kg CTIBD. Acetic acid was intravesically infused until a voiding contraction occurred; 40 min later, CTIBD was administered intraperitoneally, and micturition patterns were recorded for 90 min. Each error bar indicates S.D. One-way ANOVA followed by Tukey's post-test was used for statistical analysis. (n = 4, * *P*-value < 0.05, ** *P*-value < 0.01, *** *P*-value < 0.001.)

Downloaded from molpharm.aspetjournals.org at ASPET Journals on April 20, 2024

Molecular Pharmacology Fast Forward. Published on December 2, 2020 as DOI: 10.1124/molpharm.120.000106
This article has not been copyedited and formatted. The final version may differ from this version.

Schemes

Scheme 1. Synthesis of CTIBD. Reagents and conditions: (a) $BF_3.Et_2O$, 90^oc, 55%; (b) trifluoroacetic anhydride, pyridine, 0^oC to room temperature, 48 hours (without isolation used for next step); (c) hydroxylamine hydrochloride, pyridine, reflux, 12 hours, 51% (over two steps).

Downloaded from molpharm.aspetjournals.org at ASPET Journals on April 20, 2024

Downloaded from molpharm.aspetjournals.org at ASPET Journals on April 20, 2024

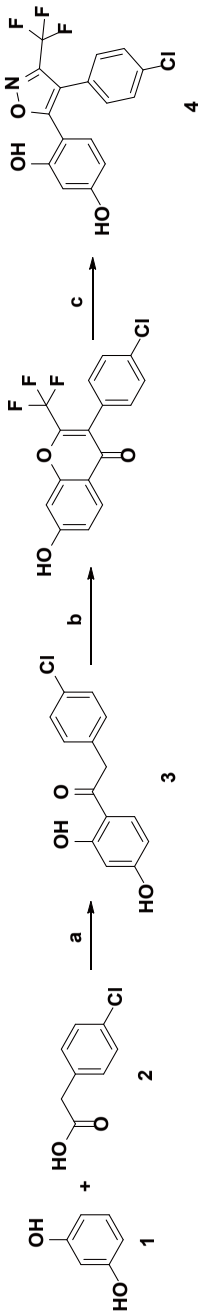

Figure 1

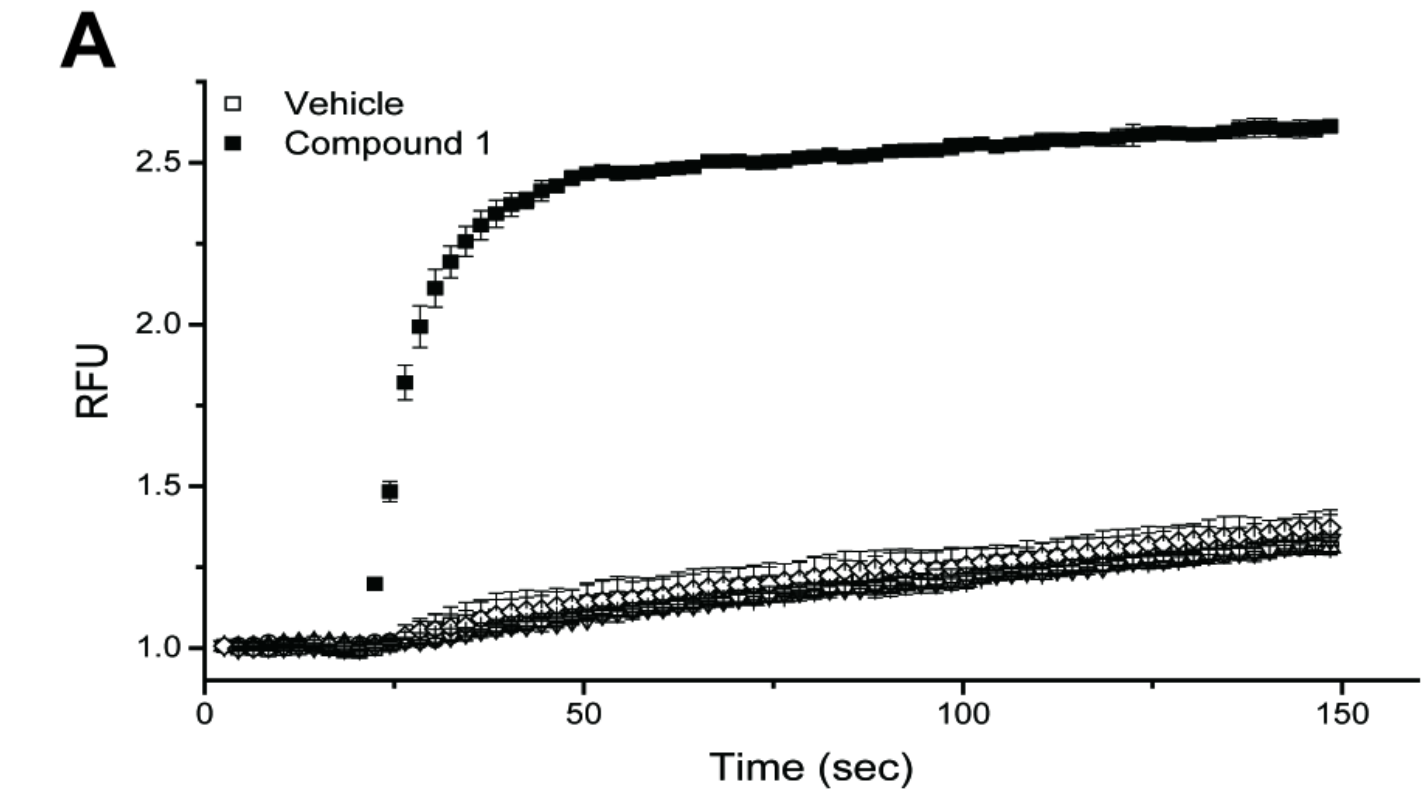

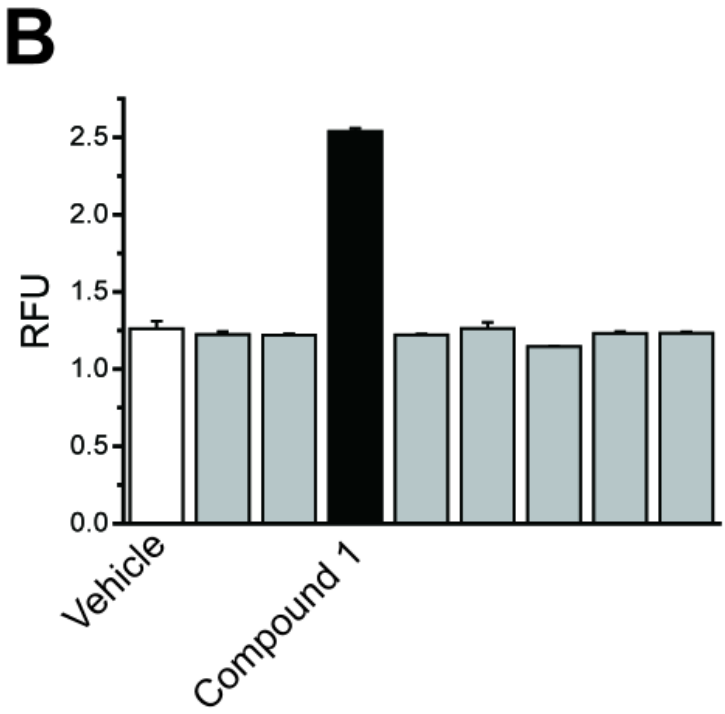

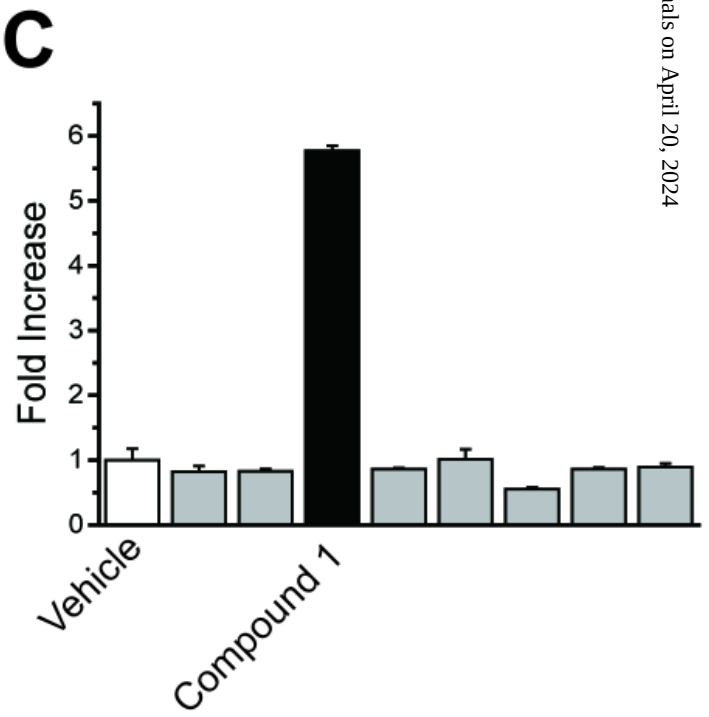

Downloaded from molpharm.aspetjournals.org at ASPET Journals on April 20, 2024

Figure 2

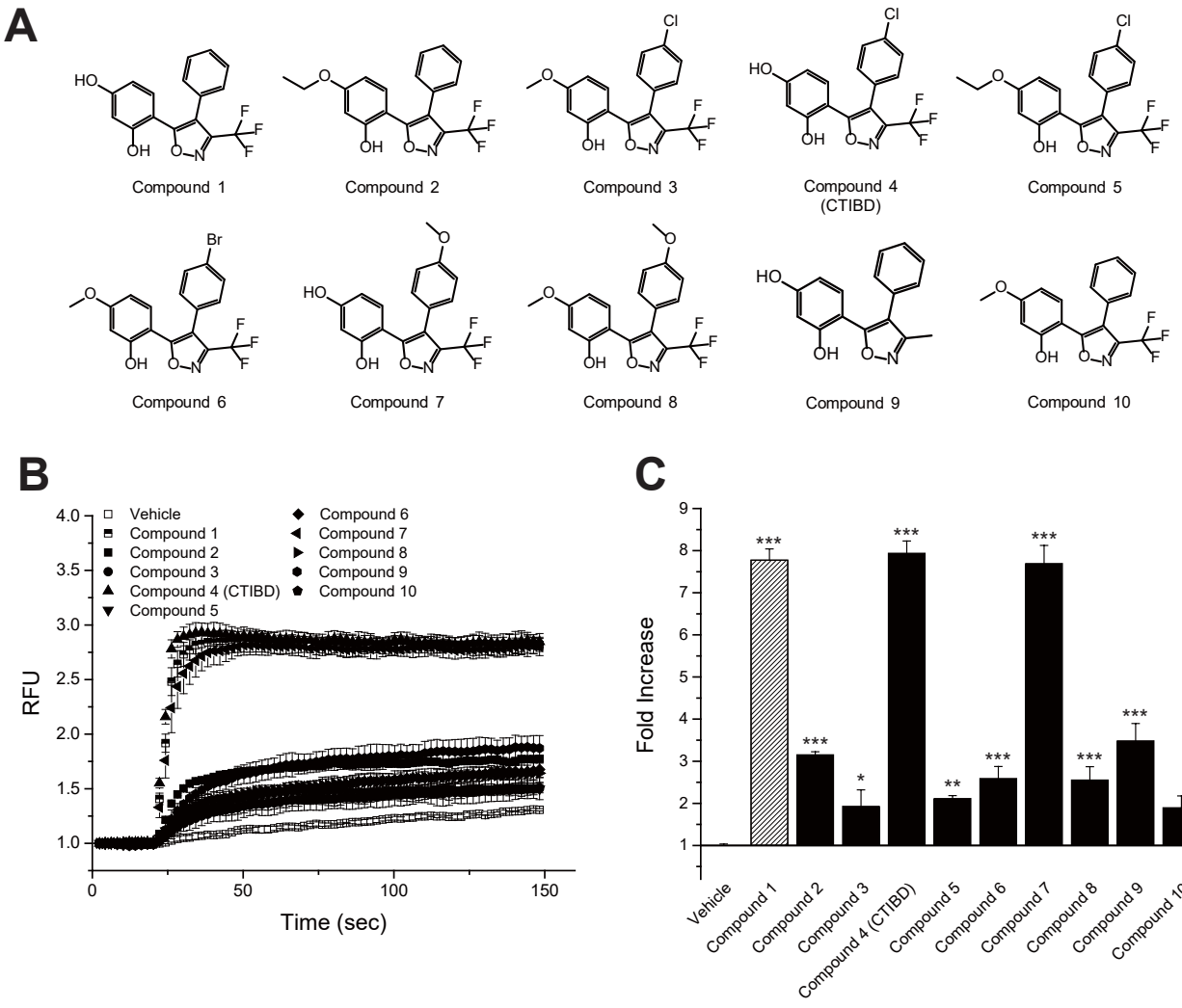

Downloaded from molpharm.aspetjournals.org at ASPET Journals on April 20, 2024

Figure 3

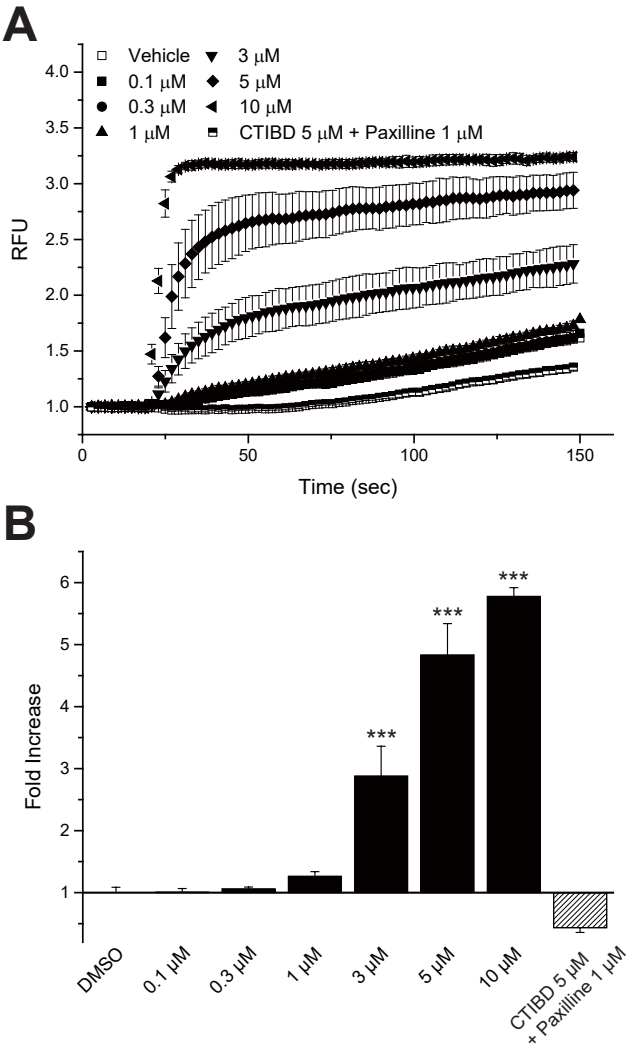

Downloaded from molpharm.aspetjournals.org at ASPET Journals on April 20, 2024

Figure 4

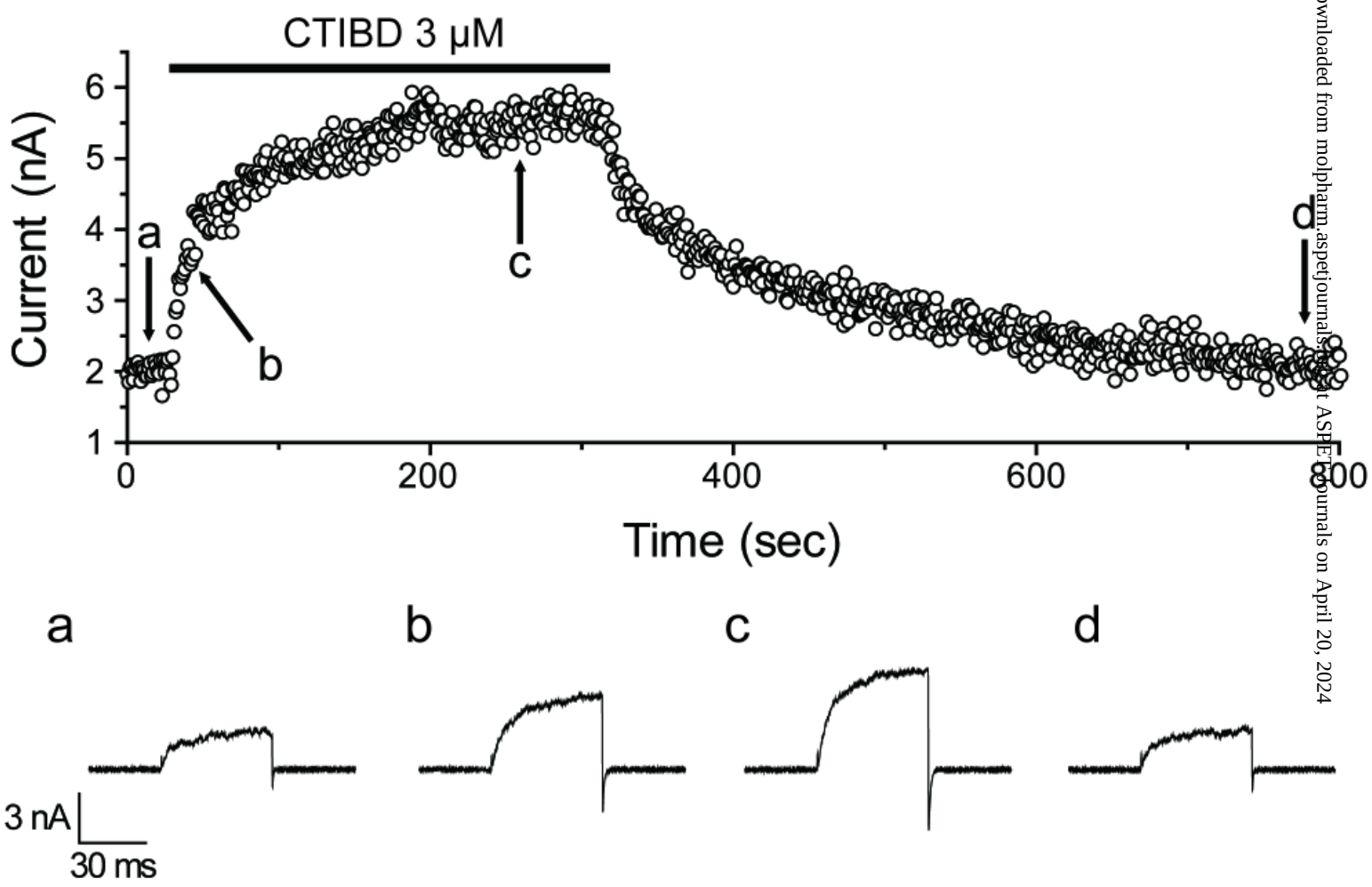

Downloaded from molpharm.aspetjournals.org at ASPET Journals on April 20, 2024

Figure 5

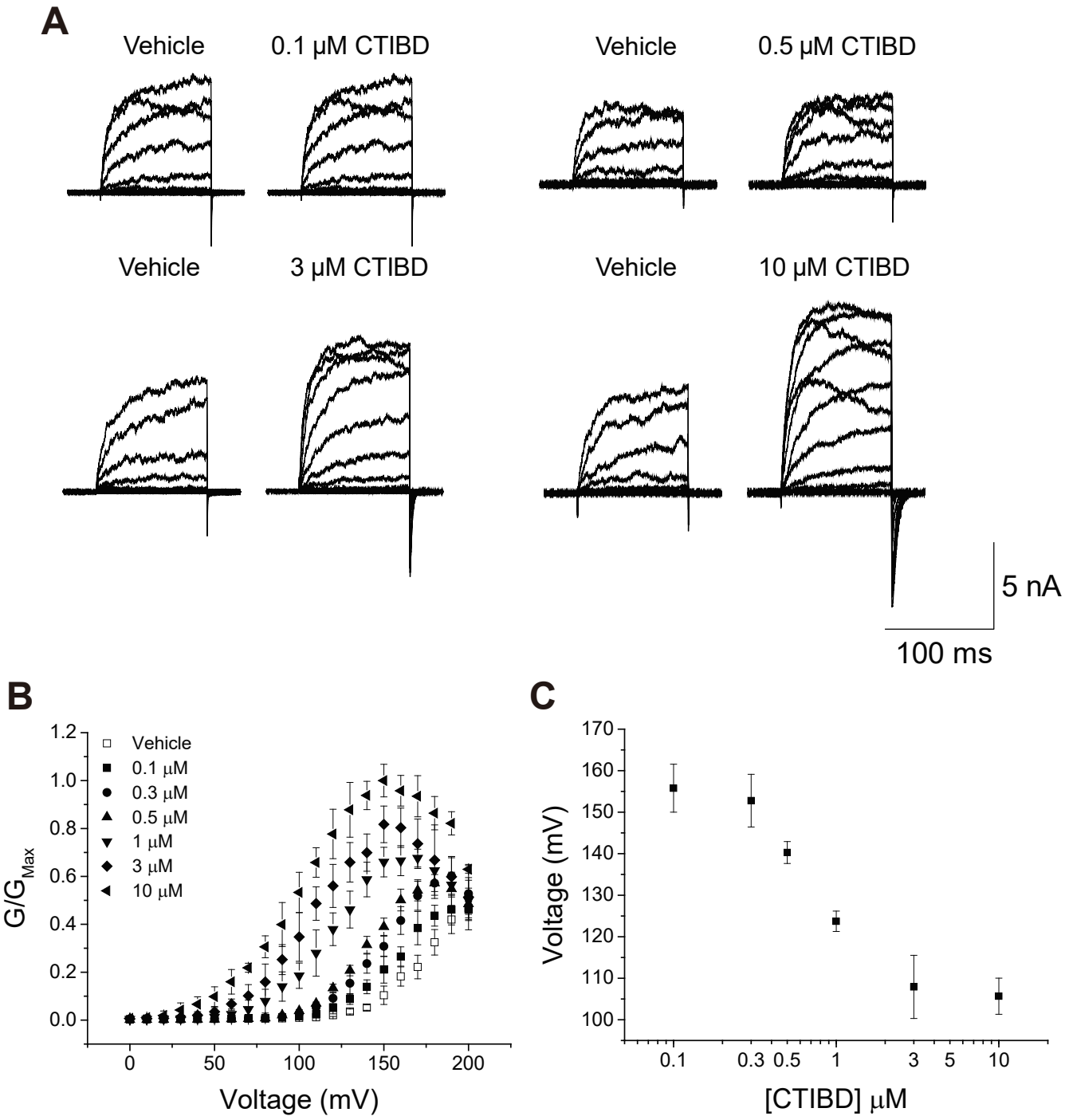

Downloaded from molpharm.aspetjournals.org at ASPET Journals on April 20, 2024

Figure 6

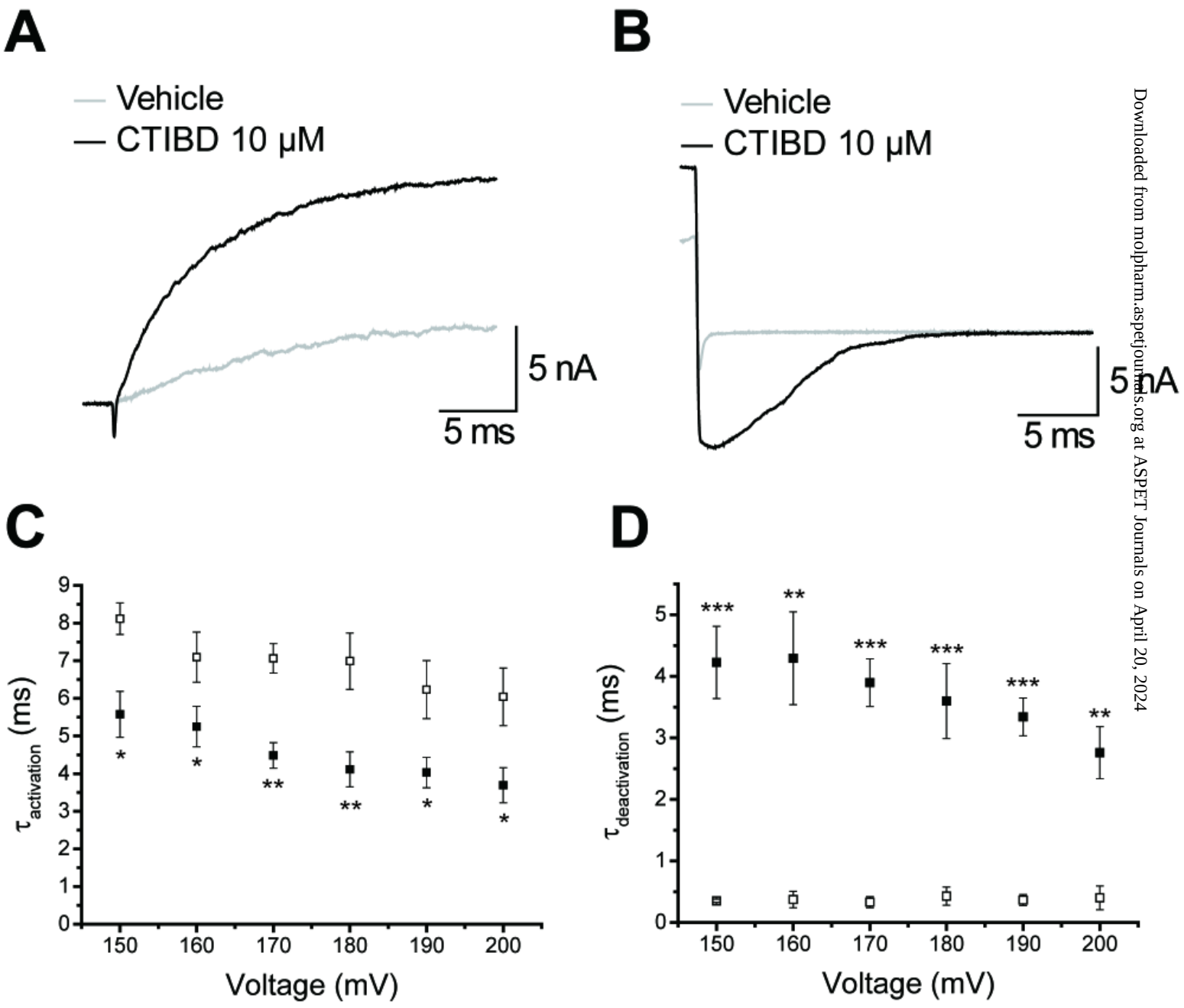

Downloaded from molpharm.aspetjournals.org at ASPET Journals on April 20, 2024

Figure 7

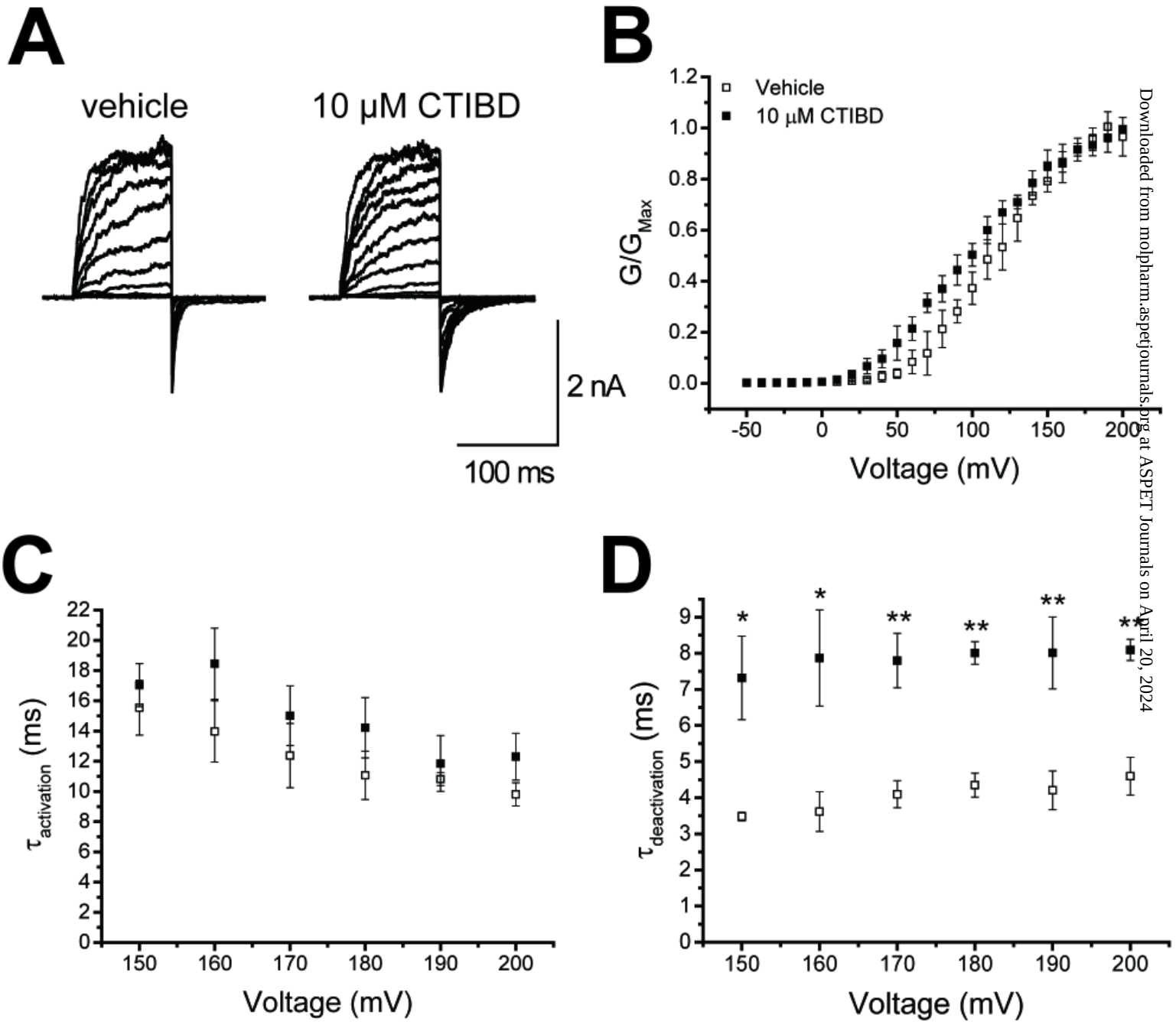

Downloaded from molpharm.aspetjournals.org at ASPET Journals on April 20, 2024

Figure 8

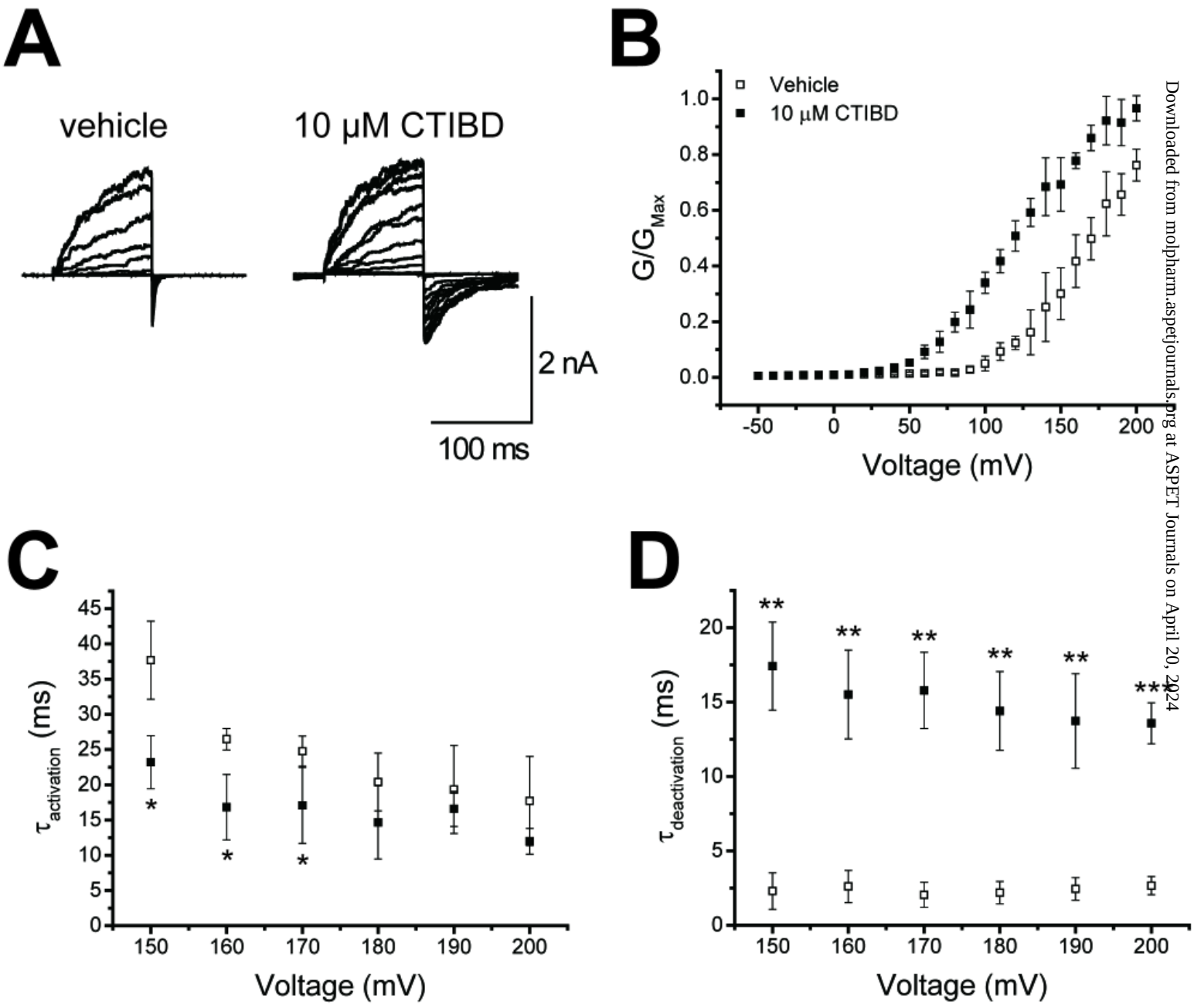

Downloaded from molpharm.aspetjournals.org at ASPET Journals on April 20, 2024

Figure 9

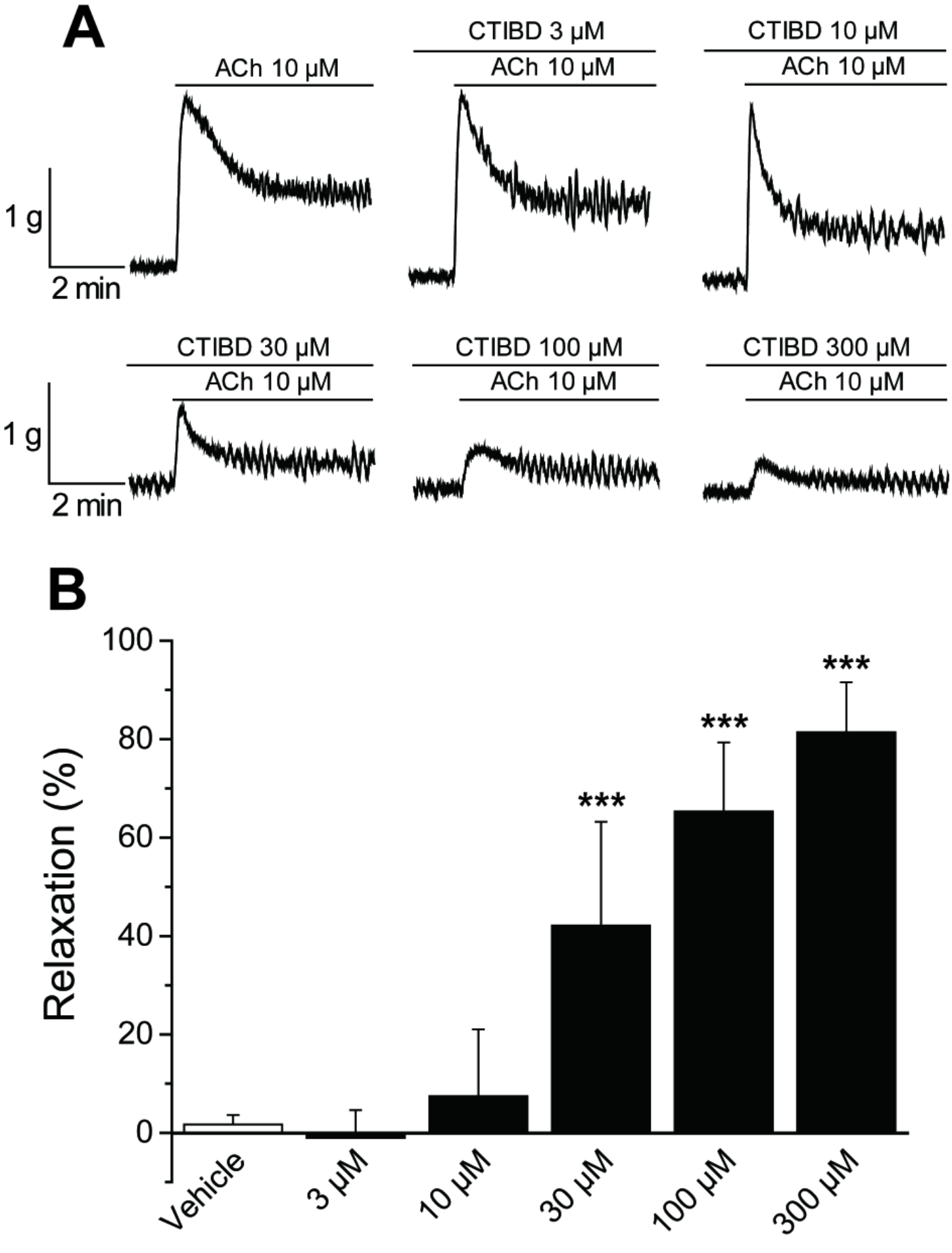

Downloaded from molpharm.aspetjournals.org at ASPET Journals on April 20, 2024

Figure 10

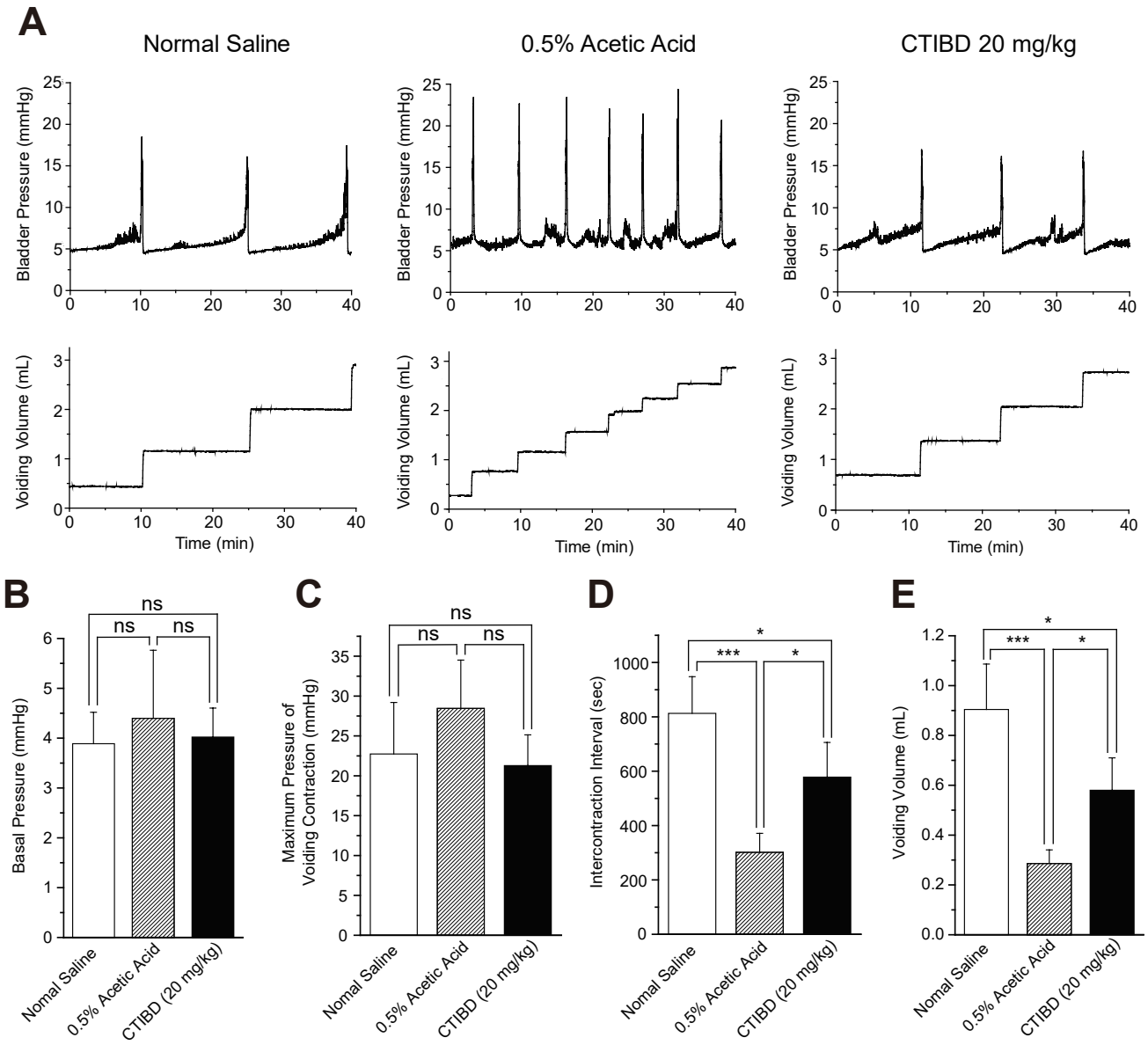

Downloaded from molpharm.aspetjournals.org at ASPET Journals on April 20, 2024

Supplemental Materials

MOLPHARM-AR-2020-000106R1

Identification and Characterization of a Novel BK_{Ca} Channel Activator, CTIBD, and Its Relaxation Effect on Urinary Bladder Smooth Muscle

Narasaem Lee, Bong Hee Lim, Kyu-Sung Lee, Jimin Shin, Haushabhau S. Pagire, Suvarna H. Pagire, Jin Hee Ahn, Sung Won Lee, Tong Mook Kang, and Chul-Seung Park*

School of Life Sciences and Center for AI-applied High Efficiency Drug Discovery, Gwangju Institute of Science and Technology (GIST), Gwangju (N.L., C.-S.P.); Department of Urology, Samsung Medical Center, Samsung Biomedical Research Institute, Sungkyunkwan University School of Medicine, Seoul (B.H.L., J.S., K.-S.L., S.W.L.); Department of Physiology, Sungkyunkwan University School of Medicine, Suwon (T.M.K.); Department of Chemistry, Gwangju Institute of Science and Technology (GIST), Gwangju (H.S.P., S.H.P., J.H.A.), Republic of Korea

Supplemental Figure 1

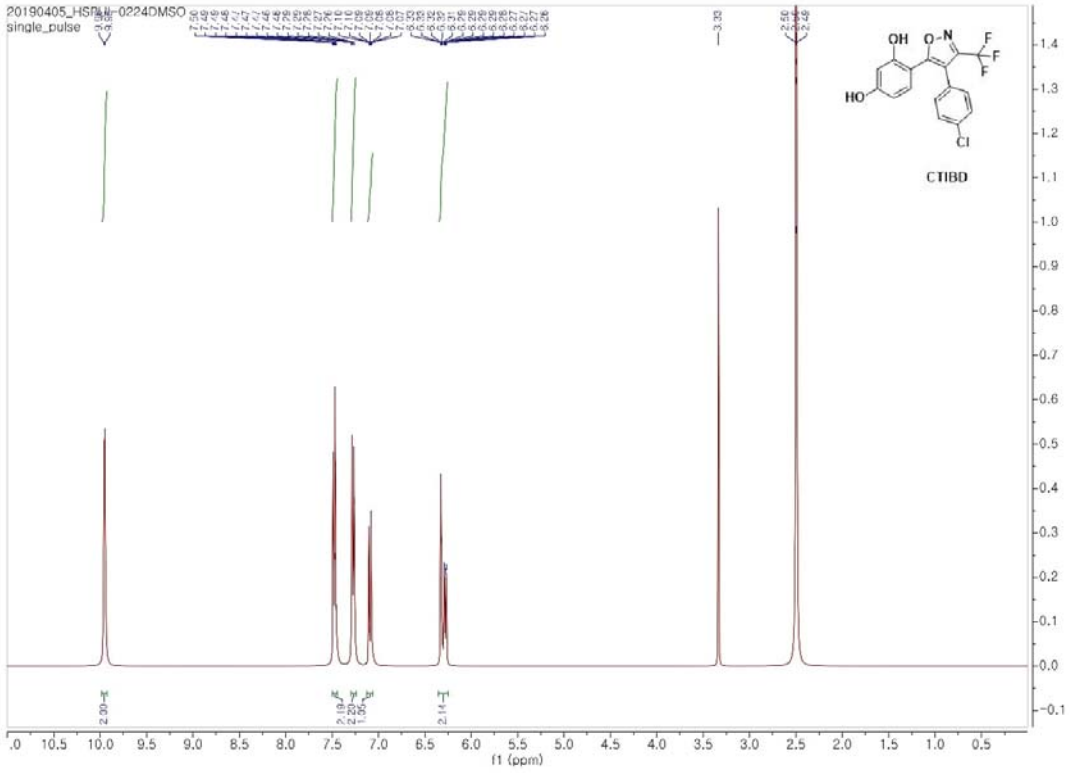

Supplemental Fig. 1. NMR data of CTIBD. ^{1}H NMR spectra were recorded on a JEOL JNM-ECS400 spectrometers at 400MHz with TMS as an internal reference. ^{1}H NMR (DMSO-d6) δ 9.96 (s, 1H), 9.95 (s,1H), 7.52-7.42 (m, 2H), 7.28 (d, J = 8.24 Hz, 2H), 7.10 (d, J = 8.24 Hz, 1H), 6.33 (d, J = 2.14 Hz, 1H), 6.28 (dd, J = 8.54, 2.14 Hz, 1H).

Supplemental Figure 2

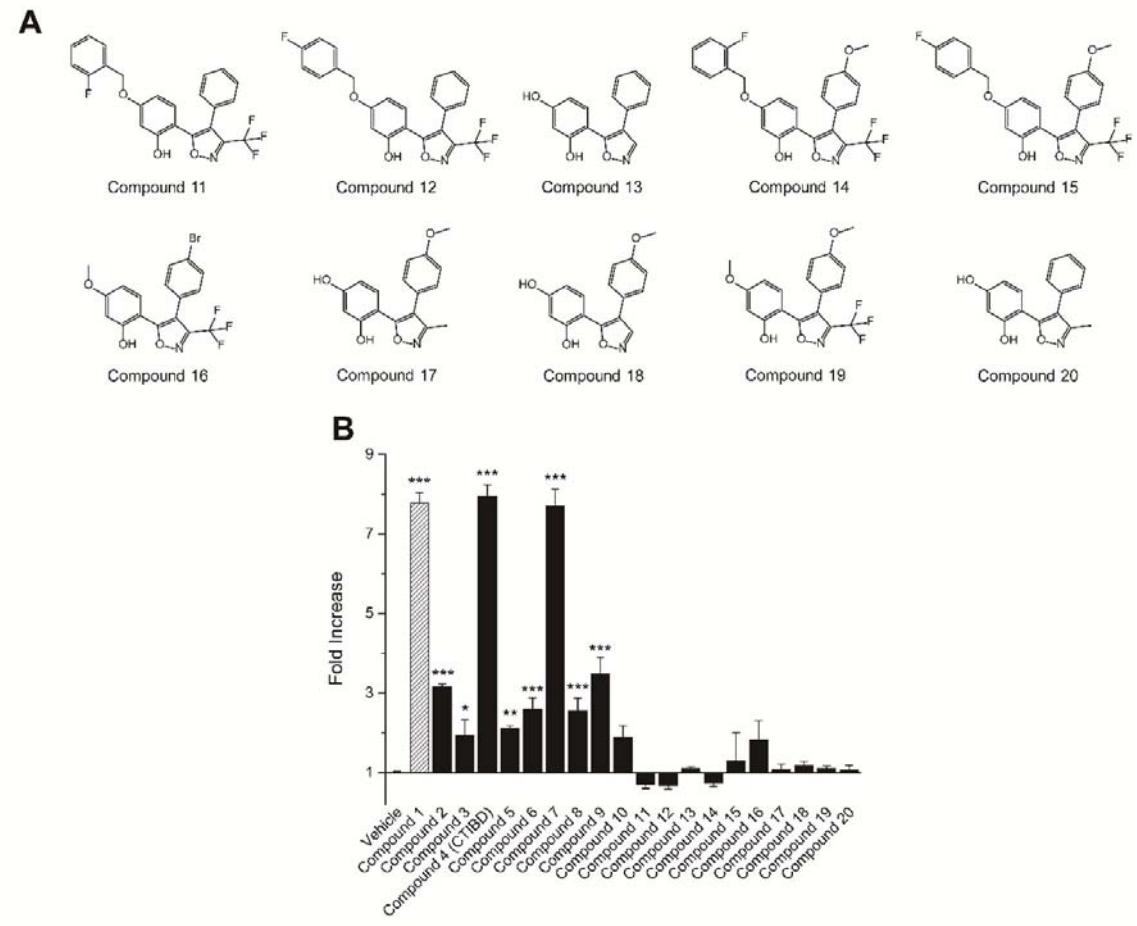

Supplemental Fig. 2. Structure–activity relationship (SAR) study centered on Compound 1. (A) Structures of compound 11 to compound 20. (B) Fold increase in RFU normalized to vehicle (1% DMSO), obtained at 100 seconds, of the 20 tested compounds are shown. Each error bar indicates S.D. One-way ANOVA followed by Dunn-Sidak's post-test was used for statistical analysis. (n = 3, * *P*-value < 0.05, ** *P*-value < 0.01, *** *P*-value < 0.001, compared with vehicle.)

Supplemental Figure 3

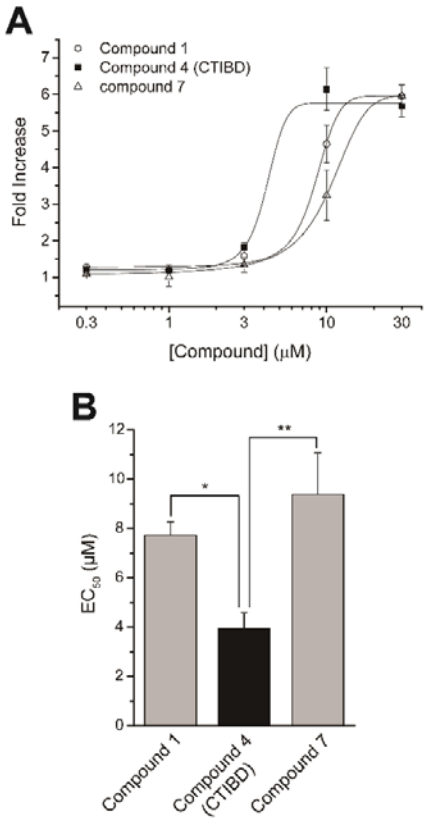

Supplemental Fig. 3. Potentiation of BK_{Ca} channel by Compound 1, Compound 4 (CTIBD), and Compound 7. (A) Fold-increase in relative fluorescence units were shown for Compound 1, CTIBD and Compound 7. Five different concentration (0.3, 1, 3, 10 and 30 μM) of each compounds are tested. The graph was fitted using the dose-response function, Fold increase = Min + (Max – Min) / (1 + 10^((EC_{50} – [Compound]) * Hill)), in the Origin 9.1 software. (B) EC_{50} value of compound 1, CTIBD and compound 7. Each error bar indicates S.D. One-way ANOVA followed by Dunn-Sidak's post-test was used for statistical analysis. (n = 3, * *P*-value < 0.05, ** *P*-value < 0.01, *** *P*-value < 0.001, compared with CTIBD.)

Supplemental Figure 4

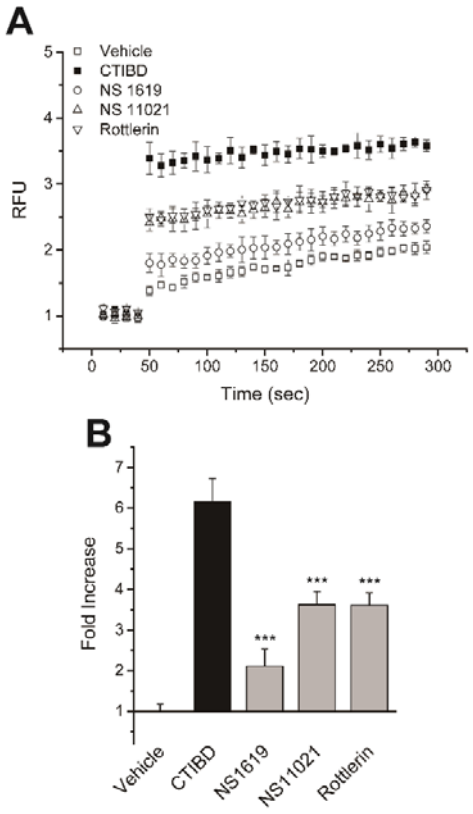

Supplemental Fig. 4. Effects of BK_{Ca} channel activators, CTIBD, NS 1619, NS 11021 and Rottlerin. (A) Representative fluorescence traces. Cells were pre-treated with vehicle (□, 1 % DMSO), CTIBD (■), NS 1619 (○), NS 11021 (△) and Rottlerin (▽) at a final concentration of 10 μM. Stimulus buffer was added at 40 seconds. (B) Fold increase in relative fluorescence units of CTIBD, NS 1619, NS 11021 and Rottlerin. Each error bar indicates S.D. One-way ANOVA followed by Dunn-Sidak's post-test was used for statistical analysis. (n = 3, * *P*-value < 0.05, ** *P*-value < 0.01, *** *P*-value < 0.001, compared with CTIBD.)

Supplemental Figure 5

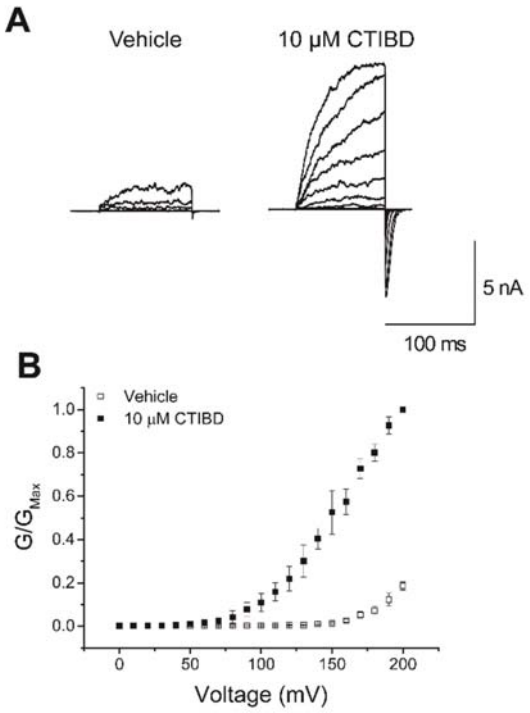

Supplemental Fig. 5. Effects of CTIBD on BK_{Ca} channel at 0.1 μM $[Ca^{2+}]_i$. (A) Representative current traces of the BK_{Ca} channel. Intracellular Ca^{2+} concentration was 0.1 μM. Vehicle was DMSO (0.1 %). 10 μM of CTIBD were applied to the extracellular side of the channel. Duration of the voltage pulses was 100 ms. Currents were recorded at every voltage pulse, which were increased from -80 to 200 mV in 10 mV increments. The holding voltage was -100 mV. Representative current traces at every 20 mV from -80 to 200 mV are shown. (B) Effects of CTIBD on the conductance–voltage relationship of the BK_{Ca} channel with 0.1 μM intracellular Ca^{2+} concentration. After initiation of voltage pulses, mean conductances were obtained from outward current values obtained between 40 and 60 ms. All currents were normalized to the maximum current obtained with 10 μM CTIBD. Vehicle (□, 0.1 % DMSO, n = 3) and 10 μM (■, n = 3) of CTIBD was applied to the extracellular side of the channel. Each error bar indicates S.D.

Supplemental Figure 6

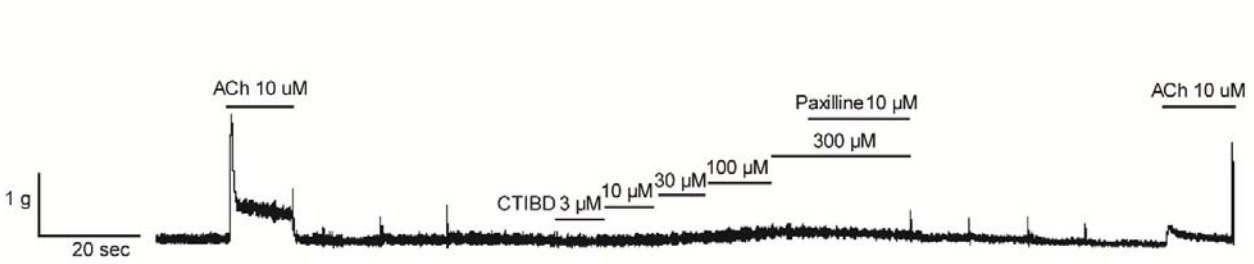

Supplemental Fig. 6. Effects of CTIBD on isolated rat urinary bladder strips without ACh-induced contraction. Representative traces of isolated rat urinary bladder strip tension is shown. 10 μM of ACh was treated to isolated bladder strip first. Then 3, 10, 30, 100 and 300 μM of CTIBD was treated. During 300 μM of CTIBD treated, 10 μM of paxilline was co-treated at the later part. 10 μM of ACh was treated to the bladder strip again at the end of recording.